

**THE USE OF STEM CELL SYNTHESIZED EXTRACELLULAR  
MATRIX FOR BONE REPAIR**

A Thesis  
Presented to  
The Academic Faculty

by

Eric R Deutsch

In Partial Fulfillment  
of the Requirements for the Degree  
Master of Science in the  
School of Mechanical Engineering

Georgia Institute of Technology  
December 2009

**THE USE OF STEM CELL SYNTHESIZED EXTRACELLULAR  
MATRIX FOR BONE REPAIR**

Approved by:

Dr. Robert Guldberg, Advisor  
School of Mechanical Engineering  
*Georgia Institute of Technology*

Dr. Evan Zamir  
School of Mechanical Engineering  
*Georgia Institute of Technology*

Dr. Todd McDevitt  
School of Biomedical Engineering  
*Georgia Institute of Technology*

Date Approved: July 16, 2009

In Memory of Joseph A. Dzialo and William L. Deutsch

## ACKNOWLEDGEMENTS

First and foremost, I would like to thank my advisor Dr Robert Guldberg. I first began working in Dr Guldberg's lab during undergrad 4 years ago. Throughout my time in the lab, Dr Guldberg has showed a lot of trust in me, allowing me to chose my own projects and design and carry out my studies as I have seen fit. This independence has helped me to grow as a researcher, learning what questions to ask and how to go about answering them. At the same time, he has been there to direct me when I was unsure of what to do or needed assistance making sense of data. His guidance and feedback were instrumental in me completing my research and growing as a researcher.

I would also like to thank my other committee members, Dr Todd McDevitt and Dr Evan Zamir. With his expertise in stem cells, Dr McDevitt provided great feedback on my planned studies. Dr Zamir's fresh perspective helped me to refine my questions and clarify my findings. They both helped to shape my research, and their advice helped me produce a better final product.

My fellow lab members have done more for me than I can possibly express, for which I am extremely grateful. Angela Lin was my mentor when I first started in the lab as an undergrad. Over the years she has not only been a great resource, especially when it comes to microCT, but she has also been a great friend. Dr Alex Peister was a post-doc in the lab during my undergrad years. She taught me everything I know about stem cells and cell culture, which was instrumental in my thesis work. When Alex left the lab for a faculty position at Morehouse, Hazel Stevens became my go to person for all things biology and cell related. Additionally, being the lab manager, she always knows where

everything is, which was extremely helpful. Ken Dupont, Joel Boerckel, and Yash Kolambkar all provided tons of help when planning and executing my *in vivo* study, which I would not have completed without them. I would also like to thank the rest of the current lab members: Mela Johnson, Chris Dosier, Jessica O'Neal, Jason Wang, Dr Liqin Xie, Dr Tamim Diab, and Brent Uhrig. Whether it was assisting with my surgeries, helping me with procedures, or just providing conversation during long hours of cell culture and pipetting, they have all been great labmates. I can only hope I was able to help them as much as they helped me. Finally I want to thank some of the lab alumni: Dr Megan Oest, Dr Craig Duvall, Dr Srinidhi Nagaraja, Dr Rhima Coleman, and Dr Blaise Porter. They were all senior lab members when I came into the lab and provided great guidance and advice.

My thanks also goes out to Dr Laura O'Farrell, Kim Benjamin, and the rest of the PRL staff. They not only kept my rats alive, but they provided great help to me during the *in vivo* studies of my research.

Finally, I would like to thank my family and friends for being there for me throughout my time at Tech. My parents, Bob and Gloria Deutsch, have provided continuous support as well as a listening ear whenever I needed to vent. I would not be where I am today without them. Along the same line, I would also like to thank my brother Kyle Deutsch, and my grandmothers Mary Dzialo and Rosemarie Deutsch. They too have been there for me from the beginning and have helped shape who I am today. In addition to my family, I would also like to express my gratitude to all my friends who have been there for me throughout the years and have provided a great release from my academic stress when I needed it. Last but certainly not least, I would like to thank my

fiancée Christina O'Neal. She has been my rock, supporting me through tough times while also sharing in my accomplishments. I cannot wait to spend the rest of my life with her!

Thank you all!!!

# TABLE OF CONTENTS

	Page
ACKNOWLEDGEMENTS	iv
LIST OF TABLES	ix
LIST OF FIGURES	x
LIST OF SYMBOLS AND ABBREVIATIONS	xiii
SUMMARY	xv
 <u>CHAPTER</u>	
1 Introduction	1
Overview	1
Background	1
Specific Aims	11
Aim 1	11
Aim 2	12
References	14
2 <i>In Vitro</i> Characterization of Stem Cell Synthesized Extracellular Matrix for Bone Tissue Engineering	20
Introduction	20
Materials and Methods	24
Stem Cell Isolation and Culture	24
Osteogenic Differentiation and Decellularization Process	25
2D Studies	27
DNA Quantification	27
Alkaline Phosphatase Activity	28

Calcium Quantification	28
3D Studies	31
3D Mineralization	34
Attachment and Proliferation	34
Statistical Analysis	36
Results	36
Decellularization	36
2D Studies	39
3D Studies	46
Discussion	55
References	59
3 <i>In Vivo</i> Evaluation of the Bone Regenerative Potential of Stem Cell Synthesized Extracellular Matrix	61
Introduction	61
Materials and Methods	63
Scaffold Preparation	63
Femoral Segmental Defect Surgery	63
X-Ray and MicroCT Analysis	64
Statistical Analysis	65
Results	68
Discussion	75
References	76
4 Conclusions and Future Work	77
Conclusions	77
Future Work	80
References	83



## LIST OF TABLES

	Page
Table 2.1: Summary of experimental groups for 2D calcium and alkaline phosphatase assays.	30
Table 2.2: Summary of experimental groups for 3D mineralization on PCL scaffolds.	35
Table 3.1: Number of bridged defects for each group at each time point, as determined from x-ray images (bridged/total).	73

## LIST OF FIGURES

	Page
Figure 2.1: MicroCT images of the side and top views of a 6 mm diameter by 9 mm thick PCL scaffold.	33
Figure 2.2: Diagram of Teflon disk with stainless steel pins used to hold scaffolds during 3D <i>in vitro</i> culture.	33
Figure 2.3: DNA content of scaffolds pre and post decellularization. Decellularization process significantly decreased cellularity of the scaffolds (n=4). * p<0.0001, error bars are ± standard error.	37
Figure 2.4: Confocal microscopy images of scaffolds pre decellularization (A-D), post decellularization (E-H), and reseeded with MSCs after decellularization (I-L). Live cells appear green and dead cells appear red. Images were taken of the exterior of the scaffolds at the top (A,E,I), bottom (C,G,K), and side (D,H,L), as well as of the interior by cutting the scaffold longitudinally (B,F,J). Scale bars are 100 µm.	38
Figure 2.5: DNA quantification of MSCs cultured on AFS cell or MSC synthesized matrix.(n=6). * p<0.05, # p<0.05 compared to week 0, \$ p<0.05 compared to week 3. Error bars are ± standard error.	42
Figure 2.6: Alkaline phosphatase activity for MSCs cultured on ECM in A) osteogenic media, B) supplemental (n=6). * p<0.05 compared to MSCs on tissue culture plastic, # p<0.05 compared to MSCs on AFS cell synthesized ECM, \$ p<0.05 compared to other time points, & p<0.05 compared to week 1, ! p<0.05 compared to week 3. Error bars are ± standard error.	43
Figure 2.7: Calcium content for cells cultured on A) AFS cell synthesized ECM, B) MSC synthesized ECM, C) tissue culture plastic (n=6). * p<0.05 compared to MSCs in osteogenic media, # p<0.05 compared to MSCs in supplemental media. Error bars are ± standard error.	44
Figure 2.8: Calcium content for MSCs cultured on ECM in A) osteogenic media, B) supplemental (n=6). * p<0.05 compared to MSCs on MSC synthesized ECM, # p<0.05 compared to MSCs on AFS cell synthesized ECM. Error bars are ± standard error.	45

Figure 2.9: 3D mineralized matrix volume produced by cells cultured on MSC synthesized ECM with preculture periods of A) 4 weeks B) 8 weeks (n=6). * p<0.05 compared to supplemental media, # p<0.05 compared to HEK cells, \$ p<0.05 compared to week 0, & p<0.05 compared to week 4. Error bars are ± standard error.	48
Figure 2.10: 3D mineralized matrix volume produced by cells cultured on AFS cell synthesized ECM with preculture periods of A) 4 weeks B) 8 weeks (n=6). * p<0.05 compared to supplemental media, # p<0.05 compared to HEK cells, \$ p<0.05 compared to week 0, & p<0.05 compared to week 4. Error bars are ± standard error.	49
Figure 2.11: 3D mineralized matrix volume produced by cells cultured on collagen coated scaffolds (n=6). * p<0.05 compared to supplemental media, # p<0.05 compared to HEK cells, \$ p<0.05 compared to week 0, & p<0.05 compared to week 4. Error bars are ± standard error.	50
Figure 2.12: 3D mineralized matrix volume produced by MSCs cultured in A) osteogenic media B) supplemental media (n=6). * p<0.05 compared to collagen coated scaffolds, # p<0.05 compared 4 week precultured MSC synthesized ECM, \$ p<0.05 compared to 8 week precultured MSC synthesized ECM, & p<0.05 compared to 4 week precultured AFS cell synthesized ECM. Error bars are ± standard error.	51
Figure 2.13: MicroCT images of 3D constructs 4 weeks following reseeding. Images are representative of the average value of mineral volume for each group at the 4 week time point. The columns show in order: reseeded MSCs cultured in osteogenic media, reseeded MSCs cultured in supplemental media, and reseeded HEK cells cultured in osteogenic media. Scale bars are 1 mm.	52
Figure 2.14: MicroCT images of 3D constructs 8 weeks following reseeding. Images are representative of the average value of mineral volume for each group at the 8 week time point. The columns show in order: reseeded MSCs cultured in osteogenic media, reseeded MSCs cultured in supplemental media, and reseeded HEK cells cultured in osteogenic media. Scale bars are 1 mm.	53
Figure 2.15: Cell attachment proficiency for MSCs reseeded onto decellularized ECM (n=4). * p<0.05 compared to cell synthesized ECM groups. Error bars are ± standard error.	54
Figure 2.16: DNA content of decellularized ECM constructs 1 day and 1 week following reseeding with MSCs (n=4). * p<0.05 compared to day 1. Error bars are ± standard error.	54
Figure 3.1: Femoral segmental defect with attached polysulfone fixation plate.	67

Figure 3.2: Volume of interest (VOI) used for microCT analysis of defect site.	67
Figure 3.3: High resolution x-ray images of rat femoral segmental defects treated with AFS synthesized ECM. Images were taken at 4 weeks (left column), 8 weeks (center column), and 12 weeks (right column). Each row corresponds to the same limb at different time points.	70
Figure 3.4: High resolution x-ray images of rat femoral segmental defects treated with MSC synthesized ECM. Images were taken at 4 weeks (left column), 8 weeks (center column), and 12 weeks (right column). Each row corresponds to the same limb at different time points.	71
Figure 3.5: High resolution x-ray images of rat femoral segmental defects treated with collagen coated scaffolds. Images were taken at 4 weeks (left column), 8 weeks (center column), and 12 weeks (right column). Each row corresponds to the same limb at different time points.	72
Figure 3.6: Mineral volume within the central 4.75 mm of the a rat femoral segmental defect treated with either AFS cell synthesized ECM, MSC synthesized ECM or collagen coated scaffolds. Error bars are $\pm$ standard error (n=10 for ECM groups, n=9 for collagen group).	73
Figure 3.7: <i>In vivo</i> microCT images of defects 4, 8, and 12 weeks post-implantation. Images are representative of the average value of mineralized matrix production for each group. Each row shows the same limb at the 3 time points. Scale bar is 1 mm.	74

## LIST OF SYMBOLS AND ABBREVIATIONS

2D	two dimensional
3D	three dimensional
$\alpha$ -MEM	$\alpha$ -minimum essential medium
AFS cell	amniotic fluid stem cell
BMP	bone morphogenetic protein
BMP-2	bone morphogenetic protein-2
DMSO	dimethyl sulfoxide
DNA	deoxyribonucleic acid
DNase	deoxyribonuclease
ECM	extracellular matrix
EDTA	ethylenediaminetetraacetic acid
FBS	fetal bovine serum
HA	hydroxyapatite
HEK cell	human embryonic kidney epithelial cell
MSC	mesenchymal stem cell
microCT	microcomputed tomography
NaOH	sodium hydroxide
PBS	phosphate buffered saline
PCL	poly- $\epsilon$ -caprolactone
PLGA	polylactic-co-glycolic acid
pNP	p-nitrophenol
pNPP	p-nitrophenyl phosphate
TCP	tricalcium phosphate

TGF- $\beta$ 3

transforming growth factor  $\beta$ 3

VOI

volume of interest

## SUMMARY

Stem cell synthesized extracellular matrix (ECM) may serve as a replacement for current bone grafting techniques. The overall goal of this thesis is to quantify the osteoinductivity of the ECM produced by human amniotic fluid stem cells (AFS cells), compare it to that of human mesenchymal stem cells (MSC), and assess its potential for use in bone tissue engineering therapies.

Each stem cell type was cultured in osteogenic media to produce the ECM, which was then decellularized via freeze/thaw cycling and DNase treatment. The success of the decellularization was confirmed with live/dead staining and DNA quantification.

A series of *in vitro* studies were performed to evaluate the characteristics of the ECM relevant to a bone tissue engineering therapy. Reseeded MSCs were able to attach to and proliferate on both ECM types in both 2D and 3D culture. In 2D, cells cultured on both ECM types showed increased levels of calcium deposition. Additionally, cells cultured on the MSC ECM showed increased alkaline phosphatase activity. A synergistic effect on osteogenic differentiation was observed when the osteoinductive factor dexamethasone was added to the culture. In 3D, both ECM types increased the mineralized matrix production of reseeded MSCs. The AFS ECM had a greater effect than the MSC ECM.

When ECM was used to treat a rat femoral segmental defect *in vivo*, it was found that each ECM type increased the rate of bridging of the defect when compared to collagen coated scaffolds. However the ECM did not have a significant effect on the volume of mineralized matrix within the defect site in this study.

# **CHAPTER 1**

## **INTRODUCTION**

### **Overview**

Bone defects may occur due to trauma, osteolytic disease, congenital malformations, or tumor resection. The current methods of treating such defects, autografts and allografts, both have their associated shortcomings. As a result, tissue engineers seek to develop a bone graft substitute that possesses the advantages of the autograft and the allograft without the drawbacks. Stem cells have the ability to differentiate into osteoblasts, making them a possibility for a bone tissue engineering treatment. However, there are several obstacles associated with implanting live cells including immunogenicity and cell survival. An alternative use of stem cells would be to use them to synthesize an extracellular matrix (ECM) which then may be used as a bone graft alternative. Studies have shown that the ECM synthesized by mesenchymal stem cells (MSCs) that are differentiating down the osteogenic pathway has the ability to induce osteogenic differentiation in other non-differentiated MSCs.[1] Amniotic fluid stem cells (AFS cells) are another stem cell type that possess high osteogenic potential. This thesis seeks to determine the osteoinductivity of AFS cell synthesized ECM, explore its effectiveness for healing a bone defect, and compare its overall potential as a bone graft substitute to that of MSC synthesized ECM.

### **Background**

Bone injuries are a common problem, with approximately 6 million fractures occurring annually in the United States.[2] The process of bone healing consists of three



stages: an initial inflammatory response, the formation of a fracture callus, and the remodeling of the callus to restore the bones original shape and strength. With adequate vascularity, the presence of osteoinductive factors, the availability of osteoprogenitor cells, and mechanical stability, bone has the unique ability to regenerate itself without scar formation.[3, 4, 5] However in some cases these conditions are not met and surgical intervention is necessary to achieve proper healing. In such cases bone grafts are required to treat the bone defect. An estimated 500,000 bone-grafting operations are performed each year in the United States to treat patients with nonunions or large defects.[6] These large defects may be the result of a variety of causes including traumatic injury, congenital malformations, osteolytic disease, tumor resection, or soft tissue damage (spinal fusions). The graft aids in the healing of these defects by providing osteoinductive and angiogenic growth factors, a source of cells capable of osteogenesis, and/or a structural matrix to impart mechanical stability.[7]

The current gold standard for treatment of large osseous defects is the autograft, where bone is harvested from another location within the patient, usually the iliac crest, and delivered to the injury site. There are many features of autografts that make them desirable for treating bone defects: they are osteoconductive and osteoinductive, they contain cells capable of osteogenesis, and they are from the patients own body and therefore avoid immune rejection.[5] However, three characteristics of autografts limit their effectiveness. First, because the iliac crest is the only significant source of autograft tissue, the amount of tissue that can be harvested is limited in quantity. Second, in many cases the harvesting procedure can result in pain and/or morbidity at the donor site. Finally, autografts do not provide structural integrity to the injury site.[8] An alternative

treatment that avoids these drawbacks is the allograft, which involves harvesting bone from a cadaver for the grafting material. This technique has the advantage of providing more graft material and structural support to the defect site. However the allograft has its own drawbacks including lack of viable cells, risk of disease transmission, poor remodeling, and inconsistencies between donors. This leads to a 25% clinical failure rate and 30-60% overall complication rate. [9, 10, 11]

Given the limitations associated with the current treatments, there is a clear need for a more refined approach to the grafting of large bone defects. The field of tissue engineering aims to develop biological substitutes to restore, maintain, or improve tissue function. To do so, it makes use of principles from both engineering and the life sciences. [12, 13] The overall goal of bone tissue engineering research is to develop a bone graft substitute that possess all the benefits of both the autograft and the allograft, without the associated limitations.[14] Successful bone regeneration requires a vascular supply, osteoinductive factors, and a source of cells capable of differentiating into osteoblasts. Tissue engineers attempt to supply one or more of these aspects to stimulate the body's natural healing response. Many of these approaches involve the use of a matrix material or scaffold that may serve several purposes: it may act as an osteoconductive surface to facilitate bone growth, a structural support to provide mechanical integrity at the defect site, a delivery vehicle to bring other factors to the injury site, or a combination of the three.[3] However, the use of a matrix material or scaffold alone has proven to be inadequate when attempting to restore function to a large bone defect.[15]

Growth factor proteins are widely studied for their use in a variety of tissue engineering applications. Each protein has highly specific actions, lending to their

usefulness.[16] Bone morphogenetic proteins (BMPs) are one family of growth factors of particular interest in bone tissue engineering.[17, 18, 19] First defined in 1965 by Marshall Urist, they have been shown to induce bone formation in both ectopic and orthotopic *in vivo* models. [20, 21, 22] Although the delivery of BMPs alone has been shown to heal a segmental defect, it takes a very high dose to do so, which risks the formation of cyst-like bone voids.[19] As a result, several methods are being developed to administer growth factors in a controlled fashion, releasing a lower dose that is sustained over a longer period of time.[23, 24] However, even with a safer, more efficient delivery method, the high cost of producing such growth factors may ultimately limit their clinical use.

Cell-based therapies comprise another promising line of research in orthopaedic tissue engineering. Cells produce the mineralized matrix that constitutes the extracellular component of bone, and therefore are ultimately responsible for bone repair. Therapies comprised of scaffolds and/or growth factors alone rely on native cells from within the host to migrate to the injury site to initiate injury repair. However in smokers, elderly patients, and patients receiving chemotherapy or radiation treatment, the endogenous osteoprogenitor cell population may be compromised, making such treatments ineffective.[25] The lack of a live cell population is thought to be one of the reasons allografts have poor remodeling and higher failure rates.[26] To account for these deficiencies, many cell-based therapies attempt to deliver live cells that are capable of osteogenesis to the defect site. A large number of cells are needed for repair of a large defect. Fully differentiated osteoblasts are therefore not an attractive option due to the large amount of time it would take to obtain an appropriate number of cells via *in vitro* expansion. Instead, cell-based therapies center on the use of stem cells. Stem cells have

two major advantages: they are highly proliferative and they can undergo osteogenic differentiation to produce bone.[27]

The source of stem cells remains a critical issue in tissue engineering. Cells from different sources have different characteristics and capabilities.[28, 29] Mesenchymal stem cells (MSCs) are the most studied cell source for orthopaedic tissue engineering. First isolated from bone marrow, MSCs were found to adhere to tissue culture plates, form spindle shapes similar to fibroblasts, and proliferate in colonies.[30, 31] Although there is some heterogeneity within this cell population, as evidenced by the various names given to subtypes over the years including bone marrow stromal cells, mesodermal progenitor cells, and connective tissue progenitors, they generally share the characteristics as being adherent and forming colonies on tissue culture plates, having a spindle shape, and having the ability to differentiate into one or more of the connective tissues.[32, 33, 34] With the proper chemical and mechanical stimuli, MSCs have shown the ability to differentiate into several different cell types including adipocytes, myocytes, chondrocytes, tenocytes, hepatocytes, epithelial cells, neural cells, and most importantly for bone tissue engineering, osteoblasts.[35, 36] Osteogenic differentiation can be induced by adding dexamethasone, ascorbic acid, and an inorganic phosphate source to the media.[37] Since their initial discovery in bone marrow they have also been found in other tissue types such as adipose tissue, synovium, trabecular bone, human umbilical cord, teeth, and lung. [38, 39]

Many studies have been done in several models to investigate the use of MSCs in a bone graft substitute. Bruder led some of the first studies to explore using bone marrow derived MSCs to heal a critically sized bone defect. In the groups initial study they

seeded cultured-expanded autologous rat MSCs on cylindrical hydroxyapatite/tricalcium phosphate (HA/TCP) scaffolds and implanted them in an 8 mm critically sized femoral segmental defect in adult rats. They found that the scaffolds containing MSCs showed better healing and a greater bone fill percentage than empty scaffolds or scaffolds containing unprocessed bone marrow.[40] A similar study was then done on a larger scale, implanting autologous MSCs on HA/TCP scaffolds into a 21 mm critically sized canine femoral segmental defect. This large animal model yielded similar results to the rat model, with the MSC loaded scaffolds showing significantly better healing than empty scaffolds or empty defects.[41] The group then turned to an allogeneic cell source to determine if the results would be similar to an autologous source. Human MSCs were seeded on HA/TCP scaffolds and implanted into 8 mm femoral segmental defects in athymic rats. The cell loaded constructs showed increased healing in comparison to empty constructs, with bone fill similar to that seen in the autologous cell scaffolds of the previous study. Additionally, mechanical testing was performed on the excised limbs, with the femurs receiving MSC loaded scaffolds showing greater strength than the femurs that received scaffolds alone.[42] Other groups have had success using MSCs derived from both bone marrow and adipose tissue to heal bone defects in a variety of small and large animal models. Bone marrow and adipose derived MSCs delivered on apatite-coated polylactic-co-glycolic acid (PLGA) scaffolds healed a critically-sized mouse calvarial defect.[43] Enhanced bone formation was observed when autologous MSCs expanded on coral granules were implanted into a sheep metatarsal defect.[44]

Although the immunogenicity of MSCs is still a topic of controversy, several studies suggest that MSCs may avoid allogeneic immune rejection via multiple

mechanisms.[45] MSCs do not appear to possess MHC class II proteins, which are potent alloantigens. This may account for some of their hypoimmunogenicity.[46, 47, 48] Other evidence suggests that MSCs can avoid immune rejection by maintaining dendritic cells in an immature state.[49] The immature dendritic cells can then silence T cells by either expanding regulatory T cell populations or by deletion.[50] In addition to regulating T cells indirectly through dendritic cells, evidence also exists that suggests that MSCs have the ability to regulate T cells via a direct method.[51] Finally, MSCs may create an immunosuppressive local environment via the secretion of soluble factors. These factors include prostaglandins, interleukin-10, and indoleamine 2,3,-dioxygenase. [52] Although some data conflicts these claims, it is thought that the observed differences are due to different cell sources and techniques used to isolate the MSCs.[52]

Despite the osteogenic capabilities and apparent hypoimmunogenicity of MSCs, there are some drawbacks associated with this cell source. A cell-based clinical treatment will most likely require a very large number of cells to effectively heal a large bone defect. However, the concentration of MSCs in healthy tissue is relatively low, and becomes even more scarce as patients age, in smokers, or in patients receiving radiation or chemotherapy treatments.[25] In addition, their *in vitro* expansion capacity is limited as they may lose multilineage differentiation capabilities due to telomere shortening.[32] As a result of these limitations, an alternative stem cell source is desirable.

Amniotic fluids stem cells (AFS cells) may offer a promising alternative to MSCs in tissue engineering.[53] Amniocentesis is routinely performed during the second trimester of pregnancy to test the fetus for chromosomal abnormalities or infections.[54] A needle is inserted through the mother's abdominal wall into the uterus and amniotic sac

and approximately 20 ml of amniotic fluid are extracted. Fetal cells are then isolated from the fluid to make various diagnoses. Researchers have found multipotent progenitor cells within this cell population.[55, 56] These cells can be isolated using ligand stem cell factor, which binds to the membrane receptor c-kit found on the cells. AFS cells have shown the ability to differentiate into cells from all three embryonic germ layers, including adipogenic, osteogenic, myogenic, endothelial, neuronal and hepatic lineages. Additionally, they can expand without feeders, are non-tumorigenic, and maintain their normal karyotype through over 250 population doublings. [56] When exposed to osteogenic media containing dexamethasone, ascorbic acid 2-phosphate, and  $\beta$ -glycerol phosphate, the AFS cells express alkaline phosphatase, osteocalcin, and precipitate calcium indicating osteogenic differentiation. In 3-D culture on poly- $\epsilon$ -caprolactone (PCL) scaffolds the cells produced extensive amounts of mineralized matrix as measured by microcomputed tomography (microCT). Additionally, AFS cells that had been precultured on PCL scaffolds in osteogenic media and then implanted ectopically in athymic rats produced a significant amount of mineralized matrix *in vivo*. [57] Unpublished data from our lab further indicates that although AFS cells show a delay in mineralized matrix production when compared to MSCs, they ultimately show greater osteogenic potential.

Several possible approaches exist for using stem cells in tissue engineering. One possibility is that they may be delivered in an undifferentiated state with differentiation cues coming from the construct or the injury site.[40] A second approach involves exposing the cells to differentiation factors *in vitro* prior to implantation so that they are in the process of differentiation prior to delivery.[57, 58, 59] Stem cells may also be

altered via gene therapy to express certain factors to aid in bone repair, such as BMPs.[60] Finally, the cells may be used to synthesize an extracellular matrix (ECM) product *in vitro* which is then decellularized and implanted into the injury site to promote healing.[1, 61] Because the last approach does not involve the implantation of live cells, it avoids many of the complications of the other cellular therapies including immunogenicity of the cells, preservation of the cells for an off-the-shelf therapy, and maintaining cell survival upon implantation.

ECM consists of a complex milieu of biologic factors and structural proteins. Not only does it provide a support structure for adherent cells, but it also acts as a localized reservoir for secreted growth factors that can be released at a later time to affect cellular behavior.[62] ECM can be decellularized through either mechanical or chemical methods, or through a combination of the two.[63, 64] Acellular matrices have been produced from a variety of tissues including intestine, bladder, skin, and heart valves.[65, 66, 67, 68] Evidence suggests that the ECM retains its bioactivity following the decellularization process.[69, 70]

Several studies have been done by the Mikos group to evaluate the use of MSC synthesized ECM in bone tissue engineering. In one study, MSCs were seeded on titanium fiber scaffolds and cultured in osteogenic media. The ECM was then decellularized via freeze-thaw cycling, reseeded with MSCs, and cultured in media lacking the osteogenic stimulus dexamethasone. The ECM was found to induce osteogenic differentiation in the reseeded MSCs, as evidenced by their increased levels of alkaline phosphatase and calcium in comparison to MSCs seeded on the titanium scaffolds alone. Additionally, when dexamethasone was added to the media a profound



synergistic effect was observed: the cells seeded on ECM with dexamethasone had much higher alkaline phosphatase and calcium levels than cells cultured on ECM without dexamethasone or cells cultured on titanium scaffolds alone with dexamethasone.[1] In a similar study, it was found that the ECM influenced the cells at the level of gene expression, causing an upregulation of genes associated with osteogenesis, coupled with a downregulation of genes associated with chondrogenesis.[71] These results may suggest that the ECM provides an optimal microenvironment for osteogenic differentiation. In addition to the observed osteoinductivity, the group also found the matrix to have some angiogenic properties. When constructs were implanted intramuscularly in rats, a greater number of blood vessels were observed in constructs that contained ECM than titanium scaffolds alone.[61]

Because differentiating stem cells create an environment that is more dynamic than that of mature osteoblasts, the ECM they create may contain a different composition of molecules that are beneficial to bone repair. The ECM composition may differ between the different stem cell types as well. AFS cells are initially in a more primitive state than MSCs. Although this causes them to take longer to differentiate, the longer differentiation time may allow them to produce greater amounts of growth factors. The ECM may promote improved osteogenic differentiation, cell attachment, proliferation, or angiogenesis. A stem cell synthesized ECM treatment for bone tissue engineering applications would have advantages over current bone graft techniques, as it circumvents having to harvest an autograft from the patient while also avoiding the risk of disease transmission and possibly the poor remodeling of allografts.

## Specific Aims

The overall goal of this thesis is to quantify the osteoinductivity of the ECM produced by human AFS cells, compare it to that of MSCs, and assess its potential for use in bone tissue engineering therapies. Due to the primitive state of stem cells, they may produce ECM that is more osteoinductive than currently used grafting treatments with less limitations. This research is novel as it explores a promising regenerative medicine technique for bone. It is significant because it seeks to establish a bone tissue engineering approach with many advantages over current grafting methods.

### **Aim 1:**

*Examine and quantify the osteoinductivity of ECM produced by osteogenically induced human AFS cells and compare it to that of human MSCs in vitro.* In order to assess the osteoinductivity of the ECM, it was first isolated from the cells that synthesized it. In a series of studies, both AFS cells and MSCs were cultured in osteogenic differentiation media for varying lengths of time to generate ECM on 2D culture dishes. The matrix was then decellularized using freeze-thaw cycling, and reseeded with cells. Human MSCs were utilized for all of the reseedings, as they are more representative of the cell type that would migrate to the injury site *in vivo*. The cells were cultured further in media containing supplements necessary for osteogenesis but no osteoinductive factors (supplemental media), as well as full osteogenic media containing dexamethasone (complete media) to examine synergistic effects. Assays were performed on the cultures at various time points to analyze them for factors associated with osteogenic differentiation. These included alkaline phosphatase, calcium, and DNA content.

Further studies evaluated the osteoinductivity of the ECM in 3D. Both cell types were cultured in osteogenic differentiation media on 3D PCL scaffolds, decellularized at various time points, reseeded with MSCs, and cultured further in both supplemental and complete osteogenic media. Microcomputed tomography was used to quantitatively monitor mineralization over time. The amount, distribution, and morphology of the ECM-induced mineralized matrix production were compared between the two cells types and between different time points of ECM production. Finally, the effect of the ECM on cellular attachment and proliferation was evaluated. PCL scaffolds containing ECM produced by either AFS cells or MSCs were loaded with MSCs and then measured for DNA content at various time points to determine both how many cells attached to the ECM constructs initially, and how rapidly those cells divided. It was hypothesized that the ECM produced by the human AFSs would be osteoinductive, and that the degree of osteoinductivity would be greater than that of the MSC-synthesized ECM due to the difference in the initial maturity levels of the cells.

**Aim 2:**

*Evaluate the bone regenerative potential of ECM produced by osteogenically induced AFS cells and compare it to that of MSCs.* In order to evaluate the bone tissue engineering potential, the ECM was utilized in a challenging critically-sized segmental defect model. Decellularized scaffolds containing ECM were created as in the 3D *in vitro* study, with the optimum ECM production time determined in Aim 1. The scaffolds were then implanted into critically-sized femoral segmental defects in nude rats. MicroCT and high resolution x-ray images were taken at four week intervals up to twelve weeks in order to monitor and quantify mineral formation and defect union. The study compared

the AFSC-synthesized ECM constructs to MSC-synthesized ECM constructs and empty PCL scaffolds. The comparisons were made based on mineral formation and bridging of the defect. It was hypothesized that the mineralization and bridging of defects containing ECM constructs would be greater than that of the empty scaffolds.

## References

1. Datta N, Holtorf HL, Sikavitsas VI, Jansen JA, Mikos AG. *Effect of bone extracellular matrix synthesized in vitro on the osteoblastic differentiation of marrow stromal cells*. *Biomaterials*, 2005. 26(9): 971-977.
2. Borrelli J, Prickett WD, Ricci WM. *Treatment of nonunions and osseous defects with bone graft and calcium sulfate*. *Clin Orthop Relat Res*, 2003. 411: 245-254.
3. Khan Y, Yaszemski MJ, Mikos AG, Laurencin CT. *Tissue engineering of bone: material and matrix considerations*. *J Bone Joint Surg Am*, 2008. 90 Suppl 1: 36-42.
4. Kalfas IH. *Principles of bone healing*. *Neurosurg Focus*, 2001. 10(4): E1.
5. Tseng SS, Lee MA, Reddi AH. *Nonunions and the potential of stem cells in fracture-healing*. *J Bone Joint Surg Am*, 2008. 90 Suppl 1: 92-98.
6. Bucholz RW. *Nonallograft osteoconductive bone graft substitutes*. *Clin Orthop Relat Res*, 2002. 395: 44-52.
7. Giannoudis PV, Dinopoulos H, Tsiridis E. *Bone substitutes: an update*. *Injury*, 2005. Suppl 3: S20-27.
8. Younger EM, Chapman MW. *Morbidity at bone graft donor sites*. *J Orthop Trauma*, 1989. 3(3): 192-195.
9. Berrey BH Jr, Lord CF, Gebhardt MC, Mankin HJ. *Fracture of allografts. Frequency, treatment, and end-results*. *J Bone Joint Surg Am*, 1990. 72(6): 825-833.
10. Lucarelli E, Fini M, Beccheroni A, Giavaresi G, DiBella C, Aldini NN, Guzzardella G, Martini L, Cenacchi A, DiMaggio N, Sangiorgi L, Fornasari PM, Mecuri M, Giardino R, Donati D. *Stromal stem cells and platelet-rich plasma improve bone allograft integration*. *Clin Orthop Relat Res*, 2005. 435: 62-68.
11. Wheeler DL, Enneking WF. *Allograft bone decreases in strength in vivo over time*. *Clin Orthop Relat Res*, 2005. 435: 36-42.
12. Langer R, Vacanti JP. *Tissue engineering*. *Science*, 1993. 260(5110): 920-926.
13. Nerem RM, Sambanis A. *Tissue engineering: from biology to biological substitutes*. *Tissue Eng*, 1995. 1(1): 3-13.
14. Guldberg RE, Oest M, Lin AS, Ito H, Chao X, Gromov K, Goater JJ, Koefoed M, Schwarz EM, O'Keefe RJ, Zhang X. *Functional integration of tissue-engineered bone*

- constructs*. J Musculoskelet Neuronal Interact, 2004. 4(4): 399-400.
15. Guldberg RE, Oest ME, Dupont K, Peister A, Deutsch E, Kolambkar Y, Mooney D. *Biologic augmentation of polymer scaffolds for bone repair*. J Musculoskelet Neuronal Interact, 2007. 7(4): 333-334.
  16. Tabata Y. *Tissue regeneration based on growth factor release*. Tissue Eng, 2003. 9 Suppl 1: S5-15.
  17. Sakou T. *Bone morphogenetic proteins: from basic studies to clinical approaches*. Bone, 1998. 22(6): 591-603.
  18. Riley EH, Lane JM, Urist MR, Lyons KM, Lieberman JR. *Bone morphogenetic protein-2: biology and applications*. Clin Orthop Relat Res, 1996. 324: 39-46.
  19. Lieberman JR, Daluiski A, Einhorn TA. *The role of growth factors in the repair of bone. Biology and clinical applications*. J Bone Joint Surg Am, 2002. 84-A(6): 1032-44.
  20. Boden SD. *The ABCs of BMPs*. Orthop Nurs, 2005. 24(1): 49-52.
  21. Wozney JM. *Bone morphogenetic proteins*. Prog Growth Factor Res, 1989. 1(4): 267-80.
  22. Oest ME, Dupont KM, Kong HJ, Mooney DJ, Guldberg RE. *Quantitative assessment of scaffold and growth factor-mediated repair of critically sized bone defects*. J Orthop Res, 2007. 25(7): 941-950.
  23. Chen RR, Mooney DJ. *Polymeric growth factor delivery strategies for tissue engineering*. Pharm Res, 2003. 20(8): 1103-1112.
  24. Lee SJ. *Cytokine delivery and tissue engineering*. Yonsei Med J, 2000. 41(6): 704-719.
  25. Bruder SP, Fox BS. *Tissue engineering of bone. Cell based strategies*. Clin Orthop Relat Res, 1999. 367 Suppl: S68-83.
  26. Zhang X, Xie C, Lin AS, Ito H, Awad H, Lieberman JR, Rubery PT, Schwarz EM, O'Keefe RJ, Guldberg RE. *Periosteal progenitor cell fate in segmental cortical bone graft transplantations: implications for functional tissue engineering*. J Bone Miner Res, 2005. 20: 2124-2137.
  27. Song L, Tuan RS. *Transdifferentiation potential of human mesenchymal stem cells derived from bone marrow*. FASEB J, 2004. 18(9): 980-982.
  28. Bianco P, Robey PG. *Stem cells in tissue engineering*. Nature, 2001. 414(6859): 118-

- 121.
29. Oreffo RO, Triffitt JT. *Future potentials for using osteogenic stem cells and biomaterials in orthopedics*. Bone, 1999. 25(2 Suppl): 5S-9S.
  30. Friedenstein AJ. *Precursor cells of mechanocytes*. Int Rev Cytol, 1976. 47:327-59.
  31. Friedenstein AJ, Deriglasova UF, Kulagina NN, Panasuk AF, Rudakowa SF, Luria EA, Ruadkow IA. *Precursors for fibroblasts in different populations of hematopoietic cells as detected by the in vitro colony assay method*. Exp Hematol, 1974. 2(2):83-92.
  32. Derubeis AR, Cancedda R. *Bone marrow stromal cells (BMSCs) in bone engineering: limitations and recent advances*. Ann Biomed Eng, 2004. 32(1): 160-165.
  33. Patterson TE, Kumagai K, Griffith L, Muschler GF. *Cellular strategies for enhancement of fracture repair*. J Bone Joint Surg Am, 2008. 90 Suppl 1: 111-119.
  34. Lodie TA, Blickarz CE, Devarakonda TJ, He C, Dash AB, Clarke J, Gleneck K, Shihabuddin L, Tubo R. *Systematic analysis of reportedly distinct populations of multipotent bone marrow-derived stem cells reveals a lack of distinction*. Tissue Eng, 2002. 8(5): 739-751.
  35. Gimble JM, Guilak F, Nuttall ME, Sathishkumar S, Vidal M, Bunnell BA. *In vitro differentiation potential of mesenchymal stem cells*. Transfus Med Hemother, 2008. 35: 228-238.
  36. Baksh D, Song L, Tuan RS. *Adult mesenchymal stem cells: characterization, differentiation, and application in cell and gene therapy*. J Cell Mol Med, 2004. 8(3): 301-316.
  37. Jaiswal N, Haynesworth SE, Caplan AI, Bruder SP. *Osteogenic differentiation of purified, culture-expanded human mesenchymal stem cells in vitro*. J Cell Biochem, 1997. 64(2): 295-312.
  38. Caplan AI, Bruder SP. *Mesenchymal stem cells: building blocks for molecular medicine in the 21<sup>st</sup> century*. Trends Mol Med, 2001. 7(6): 259-264.
  39. Musina RA, Bekchanova ES, Belyavskii AV, Sukhikh GT. *Differentiation potential of mesenchymal stem cells of different origin*. Bull Exp Biol Med, 2006. 141(1): 147-151.
  40. Kadiyala S, Jaiswal N, Bruder SP. *Culture expanded, bone marrow-derived mesenchymal stem cells regenerate a critical-sized segmental bone defect*. Tissue Eng, 1997. 3: 173-185.
  41. Bruder SP, Kraus KH, Goldberg VM, Kadiyala S. *The effect of implants loaded with*

- autologous mesenchymal stem cells on the healing of canine segmental bone defects.* J Bone Joint Surg Am, 1998. 80(7): 985-996.
42. Bruder SP, Kurth AA, Shea M, Hayes WC, Jaiswal N, Kadiyala S. *Bone regeneration by implantation of purified, culture-expanded human mesenchymal stem cells.* J Orthop Res, 1998. 16(2): 155-162.
  43. Cowan CM, Shi YY, Aalami OO, Chou YF, Mari C, Thomas R, Quarto N, Contag CH, Wu B, Longaker MT. *Adipose-derived adult stromal cells heal critical-size mouse calvarial defects.* Nat Biotechnol, 2004. 22(5): 560-567.
  44. Viateau V, Guillemain G, Bousson V, Oudina K, Hannouche D, Sedel L, Logeart-Avramoglou D, Petite H. *Long-bone critical-size defects treated with tissue-engineered grafts: a study on sheep.* J Orthop Res, 2007. 25(6): 741-749.
  45. Barry FP, Murphy JM, English K, Mahon BP. *Immunogenicity of adult mesenchymal stem cells: lessons from the fetal allograft.* Stem Cells Dev, 2005. 14(3): 252-265.
  46. Gotherstrom C, Ringden O, Tammik C, Zetterberg E, Westgren M, LeBlanc K. *Immunologic properties of human fetal mesenchymal stem cells.* Am J Obstet Gynecol, 2004. 190(1):239-245.
  47. Majumdar MK, Keane-Moore M, Buyaner D, Hardy WB, Moorman MA, McIntosh KR, Mosca JD. *Characterization and functionality of cell surface molecules on human mesenchymal stem cells.* J Biomed Sci, 2003. 10(2): 228-241.
  48. Devine SM, Hoffman R. *Role of mesenchymal stem cells in hematopoietic stem cell transplantation.* Curr Opin Hematol, 2000. 7(6): 358-363.
  49. Jiang XX, Zhang Y, Liu B, Zhang SX, Wu Y, Yu XD, Mao N. *Human mesenchymal stem cells inhibit differentiation and function of monocyte-derived dendritic cells.* Blood, 2005. 105(10): 4120-4126.
  50. Steinman RM, Nussenzweig MC. *Avoiding horror autotoxicus: the importance of dendritic cells in peripheral T cell tolerance.* Proc Natl Acad Sci USA, 2002. 99(1): 352-358.
  51. Krampera M, Glennie S, Dyson J, Scott D, Laylor R, Simpson E, Dazzi F. *Bone marrow mesenchymal stem cells inhibit the response of naïve and memory antigen-specific T cells to their cognate peptide.* Blood, 2003. 101(9): 3722-3729.
  52. Ryan JM, Barry FP, Murphy JM, Mahon BP. *Mesenchymal stem cells avoid allogeneic rejection.* J Inflamm, 2005. 2:8.
  53. Cananzi M, Atala A, DeCoppi P. *Stem cells derived from amniotic fluid: new potentials in regenerative medicine.* Reprod Biomed Online, 2009. 18 Suppl 1: 17-27.



54. Siegel N, Rosner M, Hanneder M, Freilinger A, Hengstschlager M. *Human amniotic fluid stem cells: a new perspective*. *Amino Acids*, 2008. 35(2):291-293.
55. Tsai MS, Lee JL, Chang YJ, Hwang SM. *Isolation of human multipotent mesenchymal stem cells from second-trimester amniotic fluid using a novel two-stage culture protocol*. *Hum Reprod*, 2004. 19(6): 1450-1456.
56. DeCoppi P, Bartsch G Jr, Siddiqui MM, Xu T, Santos CC, Perin L, Mostoslavsky G, Serre AC, Snyder EY, Yoo JJ, Furth ME, Soker S, Atala A. *Isolation of amniotic stem cell lines with potential for therapy*. *Nat Biotechnol*, 2007. 25(1): 100-106.
57. Peister A, Deutsch ER, Kolambkar Y, Hutmacher DW, Guldberg R. *Amniotic fluid stem cells produce robust mineral deposits on biodegradable scaffolds*. *Tissue Eng Part A*, 2009. [Epub ahead of print]
58. Castano-Izquierdo H, Alvarez-Barreto J, van den Dolder J, Jansen JA, Mikos AG, Sikavitsas VI. *Pre-culture period of mesenchymal stem cells in osteogenic media influences their in vivo bone forming potential*. *J Biomed Mater Res A*, 2007. 82(1): 129-138.
59. Sikavitsas VI, van den Dolder J, Bancroft GN, Jansen JA, Mikos AG. *Influence of the in vitro culture period on the in vivo performance of cell/titanium bone tissue-engineered constructs using a rat cranial critical size defect model*. *J Biomed Mater Res A*, 2003. 67(3): 944-951.
60. Peterson B, Zhang J, Iglesias R, Kabo M, Hedrick M, Benhaim P, Lieberman JR. *Healing of critically sized femoral defects, using genetically modified mesenchymal stem cells from human adipose tissue*. *Tissue Eng*, 2005. 11(1-2): 120-129.
61. Pham QP, Kasper FK, Mistry AS, Sharma U, Yasko AW, Jansen JA, Mikos AG. *Analysis of the osteoinductive capacity and the angiogenicity of an in vitro generated extracellular matrix*. *J Biomed Mater Res A*, 2009. 88(2): 295-303.
62. Rosso F, Giordano A, Barbarisi M, Barbarisi A. *From cell-ECM interactions to tissue engineering*. *J Cell Physiol*, 2004. 199(2): 174-180.
63. Nair R, Ngangan AV, McDevitt TC. *Efficacy of solvent extraction methods for acellularization of embryoid bodies*. *J Biomater Sci Polym Ed*, 2008. 19(6): 801-819.
64. Ngangan AV, McDevitt TC. *Acellularization of embryoid bodies via physical disruption methods*. *Biomaterials*, 2009. 30(6): 1143-1149.
65. Badylak SF, Lantz GC, Coffey A, Geddes LA. *Small intestinal submucosa as a large diameter vascular graft in the dog*. *J Surg Res*, 1989. 47(1): 74-80.
66. Chen F, Yoo JJ, Atala A. *Acellular collagen matrix as a possible "off the shelf"*

- biomaterial for urethral repair*. Urology, 1999. 54(3): 407-410.
67. Chen RN, Ho HO, Tsai YT, Sheu MT. *Process development of an acellular dermal matrix (ADM) for biomedical applications*. Biomaterials, 2004. 25(13): 2679-2686.
68. O'Brien MF, Goldstein S, Walsh S, Black KS, Elkins R, Clarke D. *The SynerGraft valve: a new acellular (nongluteraldehyde-fixed) tissue heart valve for autologous recellularization first experimental studies before clinical implantation*. Semin Thorac Cardiovasc Surg, 1999. 11(4 Suppl 1): 194-200.
69. Kropp BP, Ludlow JK, Spicer D, Rippey MK, Badylak SF, Adams MC, Keating MA, Rink RC, Birkle R, Thor KB. *Rabbit urethral regeneration using small intestinal submucosa onlay grafts*. Urology, 1998. 52(1): 138-142.
70. Xu CC, Chan RW, Tirunagari N. *A biodegradable, acellular xenogeneic scaffold for regeneration of the vocal fold lamina propria*. Tissue Eng, 2007. 13(3): 551-566.
71. Pham QP, Kasper FK, Scott Baggett L, Raphael RM, Jansen JA, Mikos AG. *The influence of an in vitro generated bone like extracellular matrix on osteoblastic gene expression of marrow stromal cells*. Biomaterials, 2008. 29(18): 2729-2739.

## CHAPTER 2

### ***IN VITRO* CHARACTERIZATION OF STEM CELL SYNTHESIZED EXTRACELLULAR MATRIX FOR BONE TISSUE ENGINEERING**

#### **Introduction**

Several *in vitro* methods exist for evaluating the efficacy of potential bone tissue engineering therapies. Many of these techniques can be applied to 2D cell cultures. One of the most common ways of evaluating osteogenic differentiation in 2D is to quantify the alkaline phosphatase activity and calcium content of the culture. Alkaline phosphatase is a hydrolase enzyme that is expressed in preosseous cells.[1] During the differentiation of MSCs down the osteogenic pathway, alkaline phosphatase activity will usually peak after 1 to 2 weeks of culture and then taper off.[2] As the cells differentiate further, they will begin to calcify the extracellular matrix to produce a bone-like ECM. The calcium content of the matrix typically increases from 2 weeks of culture onward.[2] In the 2D studies, each of these parameters were quantified at different time points to monitor the osteogenic differentiation of the reseeded cells.

In addition to inducing osteogenic differentiation, the acellular ECM may have other effects that are beneficial in bone tissue engineering applications. One such aspect that can be evaluated in 2D *in vitro* culture is the effect of the ECM on the proliferation of reseeded MSCs. If the ECM induces a stronger proliferative effect, it would be beneficial as there would then be more cells to differentiate. In contrast, if the ECM suppresses proliferation it could have a negative effect by limiting the amount of cells capable of osteogenesis. To determine the effect of the ECM on the proliferation of the

reseeded MSCs, a PicoGreen assay was used to quantify DNA, which is indicative of relative cell number, at various time points.

While 2D studies provide an easy, inexpensive way to evaluate effects of the acellular ECM on reseeded cells, they can not exclusively determine the potential of a bone tissue engineering therapy. Bone repair takes place in a large, dynamic, complex 3D environment. 3D *in vitro* studies can provide a more accurate representation of this environment for the evaluation of possible therapies. Several different scaffold types have been used for 3D culture of cells.[3] In these studies, cells were seeded on medical grade PCL scaffolds for the preculture ECM synthesis period. The scaffolds were biopsy punched out of a sheet created by fused deposition modeling with a 0, 60, 120 degree strut orientation and 85% porosity. These scaffolds have several characteristics that make them beneficial in the evaluation of bone tissue engineering therapies. They are highly porous to allow cell attachment and mass transport, they have good mechanical stability, and due to their highly organized structure there is less scaffold variability influencing the observed effects.[4] Scaffolds were coated with type I collagen to create a bioactive surface and improve cell attachment.[5, 6] When large 3D scaffolds are cultured in static conditions, there is a tendency for mineralization to occur only at the periphery of the scaffold, leaving the core empty. Therefore, scaffolds in this study were cultured on rotary rocker plates to improve mass transport within the scaffold. This has been shown to induce a more even distribution of mineral throughout the scaffold.[5]

To analyze osteogenic differentiation in the 3D samples, microCT analysis was performed. The microCT takes a series of x-ray scans that are then used to construct a 3D image of the scaffold. By picking a threshold value that excludes the scaffold material,

cells, and soft tissue, the mineralized matrix produced by the cells could be isolated and quantified. These scans were taken at several time points to monitor the production over time. Multiple scans can safely be made of each scaffold, as the microCT has been shown to have no significant effect on cell mediated mineralization potential.[5, 7, 8] In addition to the microCT scans to evaluate osteoinductivity, the DNA was also quantified for the 3D scaffolds using the PicoGreen assay to assess the effect of the 3D ECM on cell attachment and proliferation.

Two different media types were used to culture the reseeded MSCs. The first was “osteogenic media”, which is supplemented with dexamethasone,  $\beta$ -glycerol phosphate, and ascorbic acid 2-phosphate. Of these three components, the dexamethasone is the primary osteoinductive agent, with the other two components supplementing the differentiating cells, but not inducing osteogenic differentiation themselves. If dexamethasone is removed from this media, cells cultured on tissue culture plastic will not osteogenically differentiate in significant numbers as they lack an osteoinductive agent. However, if another osteoinductive agent such as BMP is added to the culture they will experience differentiation. Cells were cultured with osteogenic media on the ECM to determine if there was a synergistic effect as has been seen in other studies.[9] The second media type used was referred to as “supplemental media”, which is similar to the osteogenic media but does not contain dexamethasone. It therefore will not induce osteogenic differentiation itself. This media was used to test if the ECM itself was osteoinductive.

In order to isolate the effect of the acellular ECM on the reseeded MSCs, it is imperative that the ECM be fully decellularized. Several chemical agents have been used

to decellularize matrices. These include acid/alkaline treatments such as peracetic acid, ionic detergents including sodium dodecyl sulfate, non-ionic detergents like Triton-X 100, or enzymatic treatments such as trypsin and DNase.[10] While these techniques are able to decellularize tissue, they usually require several long incubation periods and washes. Additionally, they may inadvertently remove desirable ECM components. As an alternative, mechanical techniques such as freeze/thaw cycling and lyophilization can be applied to disrupt cellular membranes.[11] While these can successfully devitalize a tissue, they do not completely remove cellular debris. In previous studies evaluating the osteoinductivity of MSC synthesized ECM, freeze/thaw cycling was used as the decellularization technique. This method was initially attempted in this study. However, it was found that a significant amount of DNA remained entrapped within the ECM following decellularization, making it impossible to accurately assess cell attachment and proliferation. The freeze/thaw cycling was therefore followed up with DNase treatment to fully decellularize the ECM.

The goal of this aim was to use *in vitro* techniques to characterize the effect of stem cell synthesized ECM on reseeded MSCs. More specifically, it set out to compare AFS cell synthesized ECM to MSC synthesized ECM in terms of its capability as a bone tissue engineering treatment. It was hypothesized that the ECM produced by the human AFS cells would be osteoinductive, and that the degree of osteoinductivity would be greater than that of the MSC-synthesized ECM due to the difference in the initial maturity levels of the cells.

## Materials and Methods

### Stem Cell Isolation and Culture

The Institute for Regenerative Medicine at Wake Forrest University graciously provided the human AFS cells used in these studies. Amniotic fluid was obtained via amniocentesis, and stem cells expressing the membrane receptor c-kit were isolated via immunoselection using an antibody for CD117.[12] The cells were then expanded at 37°C, 5% humidified CO<sub>2</sub> in  $\alpha$ -MEM supplemented with 15% FBS, 2 mM L-glutamine, 100 units penicillin, 100  $\mu$ g streptomycin (all Invitrogen, Carlsbad, Ca), 18% Chang B, and 2% Chang C (Irvine Scientific, Santa Ana, CA), which will be referred to as “AFS expansion media”.[12] Media was changed every 3 to 4 days during culture. Cells were received at passage 14 and were then passaged another 2 to 3 times before use, reaching no more than 70% confluence on each expansion. For storage, cells were frozen in AFS expansion media supplemented with 5% DMSO. For use, cells were rapidly thawed at 37°C and seeded on 150mm culture plates (BD Falcon, San Jose, CA) in AFS expansion media at a concentration of 100,000 cells per plate. Cells were harvested once they reached 70% confluence (approximately 1 week) by treating them with 0.25% trypsin-EDTA (Invitrogen).

Human MSCs were obtained from Tulane Center for Gene Therapy through the NIH-funded center for preparation and distribution of adult stem cells (2P40RR017447-06). 2 ml bone marrow aspirates were taken from the iliac crest of healthy human donors.[13, 14] Cells were isolated from these aspirates and expanded on tissue culture dishes (Nuncleon  $\Delta$  surface, Thermo Fisher, Rochester, NY) at 37°C, 5% humidified CO<sub>2</sub> in  $\alpha$ -MEM medium supplemented with 17% FBS (Atlanta Biologicals), 2mM L-

glutamine, 100 units penicillin, 100  $\mu\text{g}$  streptomycin (all Invitrogen), which will be referred to as “MSC expansion media”. Media was changed every 3 to 4 days during culture. Cells were not allowed to reach more than 70% confluence. For storage, cells were frozen in  $\alpha$ -MEM supplemented with 30% serum and 5% DMSO. For use, cells were rapidly thawed at 37°C and seeded on 100 mm culture plates (Nuncleon  $\Delta$  surface, Thermo Fisher, Rochester, NY) in MSC expansion media. After 24 hours the cells were treated with 0.25% trypsin-EDTA to remove them from the plate, counted, and reseeded at a density of 50 cells/cm<sup>2</sup> on 150 mm culture plates (Nuncleon  $\Delta$  surface, Thermo Fisher, Rochester, NY) in MSC expansion media. Cells were harvested once they reached 70% confluence (approximately 7-10 days) by treating them with 0.25% trypsin-EDTA.

### **Osteogenic Differentiation and Decellularization Process**

To differentiate the MSCs and the AFS cells down the osteogenic lineage, the cells were cultured in MSC expansion media further supplemented with 1  $\mu\text{M}$  dexamethasone, 3 mM  $\beta$ -glycerol phosphate, 50  $\mu\text{g/ml}$  ascorbic acid 2-phosphate, and 50ng/ml thyroxine (all Sigma, St Louis, Missouri), which will be referred to as “osteogenic media”. [15, 16] The media was changed every 3 to 4 days during the differentiation period. Once the cells had been cultured for the desired time period, the ECM was decellularized using a combination of mechanical and chemical means.[9, 10, 11] First, the cells were subjected to rapid freeze/thaw cycling to disrupt the cellular membranes. For the 2D studies on tissue culture plates, the cultures were frozen in a -80 °C freezer for 20 minutes and then thawed at room temperature for 20 minutes. This process was repeated three times. For the 3D studies on PCL scaffolds, the constructs were placed in 1.5 ml micro-centrifuge tubes. The tubes were then immersed in



isopropanol at -80 °C for 20 minutes to freeze the constructs, followed by immersion in 37 °C water to thaw. This was repeated 3 times. The freeze/thaw cycling was followed with DNase treatment (Worthington Biochemical Corporation, Lakewood, NJ) to remove some cellular debris. The ECM was exposed to 1 mg/ml DNase for 30 minutes at 37 °C, followed by rinsing in PBS three times.

Successful decellularization was confirmed via two methods. First, a PicoGreen DNA quantification kit (Invitrogen) was used to measure the amount of DNA within the PCL scaffolds both before and after the decellularization process. Scaffolds were treated with 0.125 mg/ml Proteinase K (Worthington Biochemical Corporation) for 24 hours at 45 °C, followed by 2 hours at 60 °C to digest the ECM and cell membranes and release the DNA into solution. Samples were then diluted 1:20 in Tris-EDTA assay buffer. Lambda DNA standards were produced from 1 µg to 1 ng. 100 µl from each sample were added to 100 µl of PicoGreen working solution in black 96-well plates. After a 5 minute room temperature incubation period, the fluorescence was read at an excitation of 485 nm and an emission of 535 nm (Perkin-Elmer HTX 7000 fluorescent plate reader, Waltham MA) (n=4).

In addition to quantifying the DNA within the scaffolds, a Live/Dead Viability/Cytotoxicity kit (Molecular Probes, Invitrogen) was used to assess decellularization throughout the scaffolds. Scaffolds were washed three times in PBS, incubated for 45 minutes in 4 µM Ethidium homodimer-1 and 4 µM Calcein AM, and washed three additional times in PBS. Scaffolds were then viewed using a confocal microscope (LSM 510 UV, Carl Zeiss, Thornwood, NY). Images were taken at random of the top, bottom, side, and interior (by making a longitudinal cut) of the scaffolds. In

addition to images of the scaffolds pre and post decellularization, images were also made of scaffolds that had been reseeded with MSCs to examine the efficiency and distribution of the reseeded.

## **2D Studies**

For 2D studies, MSCs or AFS cells were seeded on 24-well culture dishes at a concentration of 10,000 cells/cm<sup>2</sup> in MSC expansion media. After three days the media was switched over to osteogenic media, which was then changed every 3 to 4 days. At 3 weeks from the initial seeding the cultures were decellularized as described, leaving the intact ECM. MSCs were then reseeded onto the ECM and cultured in the appropriate media until samples were collected for analysis.

### DNA Quantification

A PicoGreen DNA quantification assay was performed to assess how effectively the reseeded MSCs populated and proliferated on the ECM in 2D. ECM was produced as described and reseeded with MSCs. The reseeded samples were cultured in MSC growth media, changed every 3 to 4 days. Two cellular groups and two acellular control groups were included: MSCs cultured on MSC synthesized ECM, MSCs cultured on AFS cell synthesized ECM, MSC synthesized ECM without reseeded cells, and AFS cell synthesized ECM without reseeded cells. Samples were collected in 500 µl of 0.05% Triton-X100 (Sigma-Aldrich, St Louis, MO) in PBS at 24 hours, 1 week, 2 weeks, and 3 weeks following reseeded. DNA was quantified using the PicoGreen kit as previously described (n=6).

### Alkaline Phosphatase Activity

Alkaline phosphatase content was assessed in 2D culture using an assay to measure its activity. Samples were prepared as previously stated. Groups included ECM synthesized by each cell type reseeded with MSCs and then cultured in either osteogenic media or “supplemental media”, which consists of MSC expansion media further supplemented with 6 mM  $\beta$ -glycerol phosphate, 50  $\mu$ g/ml ascorbic acid 2-phosphate, and 50ng/ml thyroxine (no dexamethasone). Additionally, two control groups consisted of ECM produced by each cell type and reseeded with human embryonic kidney epithelial cells (HEK cells) in osteogenic media. These cells have been shown to be incapable of mineralized matrix production, and therefore served as a cellular negative control.[17] Both cell types and media conditions were also analyzed on tissue culture plastic for comparison. A summary of the experimental groups can be seen in Table 2.1. Samples were collected in 500  $\mu$ l of 0.05% Triton-X100 in PBS at 24 hours, 1 week, 2 weeks, and 3 weeks. Alkaline phosphatase activity was determined by incubating the samples with p-Nitrophenyl phosphate (pNPP) and measuring how much p-Nitrophenol (pNP) was produced via the enzyme hydrolyzing the phosphate group off of the pNPP. pNP standards were created varying from 800 to 12.5  $\mu$ M. 50  $\mu$ l of each sample were added to 50  $\mu$ l of working solution containing 20 mM pNPP and incubated at 37 °C for 1 hour. Absorbance was determined at 405 nm with a plate reader (PowerWave XS, BioTek, Winooski, VT) (n=6).

### Calcium Quantification

The amount of calcium present within the ECM produced by the reseeded cells was assessed using a calcium quantification assay. Groups, culture conditions, and

sample collection times were the same as used for the alkaline phosphatase assay. Samples were collected in 1 N acetic acid and incubated at room temperature overnight. They were then diluted 1:20 in 1 N acetic acid. 25  $\mu$ l of diluted sample were added to 300  $\mu$ l of calcium reagent (Arsenazo III, Diagnostic Chemicals Limited) in clear 96-well plates and incubated for 30 seconds at room temperature. Absorbance was determined at 615 nm with a plate reader (n=6).

Table 2.1: Summary of experimental groups for 2D calcium and alkaline phosphatase assays.

Group	Matrix Type	Cell Type for Reseed	Culture Media
1	AFS-synthesized	MSC	Osteogenic
2	MSC-synthesized	MSC	Osteogenic
3	Collagen	MSC	Osteogenic
4	AFS-synthesized	MSC	Supplemental
5	MSC-synthesized	MSC	Supplemental
6	Collagen	MSC	Supplemental
7	AFS-synthesized	HEK	Osteogenic
8	MSC-synthesized	HEK	Osteogenic
9	Collagen	HEK	Osteogenic

### 3D Studies

For 3D studies, cells were seeded on PCL scaffolds and cultured in a dynamic environment. Using fused deposition modeling, 100 mm x 100 mm by 9 mm thick sheets of PCL were created with a 0, 60, 120 degree strut orientation and 85% porosity.[4] A 6 mm biopsy punch was used to create cylindrical scaffolds from the sheet measuring 6 mm diameter by 9 mm thick (Figure 2.1). Scaffolds were incubated at 37 °C for 1 hour in 5 M NaOH to increase surface roughness.[5] They were then rinsed 5 times in deionized water and sterilized by immersion in ethanol, which was allowed to evaporate overnight.

A collagen network was created within the pores of the scaffold in order to improve cell attachment.[5, 6] 100 parts of 1.5 mg/ml type I rat tail collagen in 0.05% acetic acid was combined with 9 parts of 71.2 mg/ml sodium bicarbonate solution. 220 µl of the solution was placed into a 6 mm diameter by 10 mm deep cylindrical mold. Scaffolds were then inserted into the mold, immersing them in the collagen solution. The collagen was allowed to gel for 30 minutes at room temperature. The constructs were frozen in the mold at -80 °C for 1 hour and then lyophilized overnight. For cell seeding and culture, the scaffolds were removed from the mold and inserted into holders consisting of a ¾ inch diameter Teflon disk with 4 stainless steel pins forming a perimeter around the scaffold (Figure 2.2). The holders were designed to maintain the orientation of the scaffold during dynamic culture. The scaffolds and holders were then placed in 12-well tissue culture plates (Nunc, low cell binding surface).

Two million cells were resuspended in 200 µl of the appropriate expansion media and added drop-wise to the top surface of the collagen coated scaffolds. The media was readily absorbed by the collagen throughout the scaffold. The scaffolds were then

incubated for 1 hour at 37 °C to allow for cellular attachment. 4 ml of expansion media were then added to each well and the constructs were cultured at 37 °C. After 3 days the constructs were switched over to osteogenic media, which was then changed every 3 to 4 days, and cultured on an orbital shaker (Belly Button® orbital shaker, 7.5 rpm, minimal pitch, Stovall, Greensboro, NC) to improve mass transport within the inner regions of the constructs.[5, 18]

After the indicated preculture period, the ECM was decellularized via freeze/thaw cycling and DNase treatment as described. To facilitate reseeding throughout the 3D scaffolds, they were lyophilized following the decellularization treatment to remove liquid within the scaffold and allow media containing cells to spread throughout. The ECM containing scaffolds were then reseeded with MSCs using the same procedure as the initial seeding.

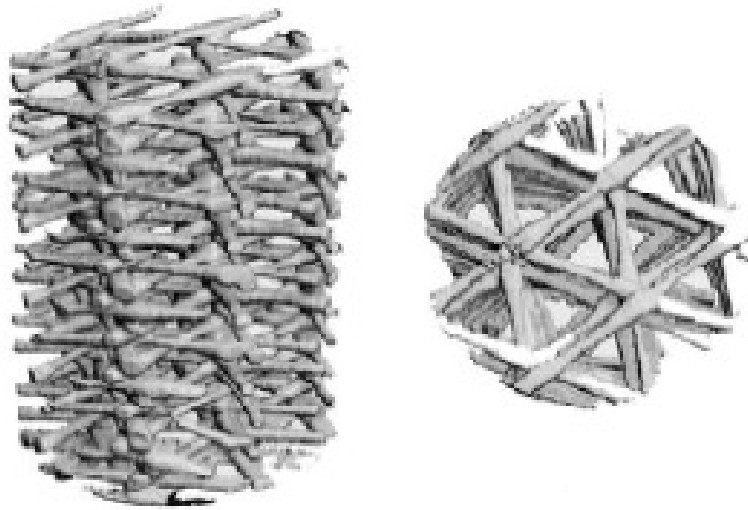


Figure 2.1: MicroCT images of the side and top views of a 6 mm diameter by 9 mm thick PCL scaffold.

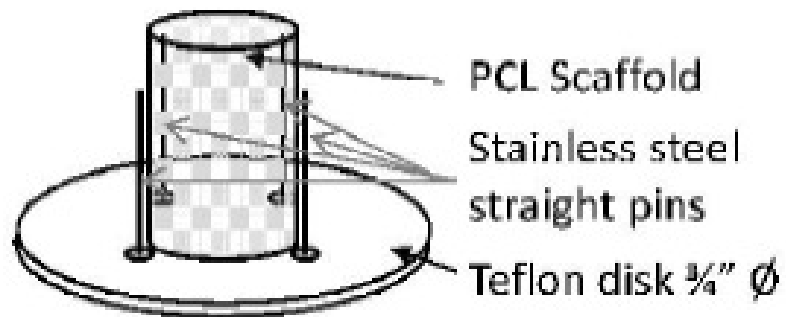


Figure 2.2: Diagram of Teflon disk with stainless steel pins used to hold scaffolds during 3D *in vitro* culture.



### 3D Mineralization

Mineralized matrix production within the constructs was assessed using microcomputed tomography (microCT). Table 2.2 summarizes the experimental groups for the 3D mineralization study. ECM was synthesized by each cell type for either 4 or 8 weeks for comparison between different preculture periods. Reseeded MSCs were cultured in either osteogenic or supplemental media. As controls, MSCs were cultured on collagen coated scaffolds in each media type and HEK cells were cultured on each matrix type. Scaffolds were microCT scanned at 0, 4, and 8 weeks in a sterile scanning chamber. They were scanned at a 38  $\mu\text{m}$  voxel resolution (VivaCT scanner, Scanco Medical, Switzerland). Scans were evaluated at a threshold of 80, a filter width of 1.2, and a filter support of 2 (n=6).[5]

### Attachment and Proliferation

Cell attachment efficiency on 3D ECM constructs was evaluated via DNA quantification. Constructs were prepared and reseeded with MSCs as in the 3D mineralization study. 1 day and 1 week after reseeding scaffolds were collected, treated with Proteinase K, and analyzed using a PicoGreen DNA quantification kit as previously described.

Table 2.2: Summary of experimental groups for 3D mineralization on PCL scaffolds.

Group	Matrix Type	Matrix Preculture Period	Cell Type for Reseed	Culture Media
I	AFS-synthesized	4 Weeks	MSC	Osteogenic
II	AFS-synthesized	8 Weeks	MSC	Osteogenic
III	MSC-synthesized	4 Weeks	MSC	Osteogenic
IV	MSC-synthesized	8 Weeks	MSC	Osteogenic
V	Collagen	N/A	MSC	Osteogenic
VI	AFS-synthesized	4 Weeks	MSC	Supplemental
VII	AFS-synthesized	8 Weeks	MSC	Supplemental
VIII	MSC-synthesized	4 Weeks	MSC	Supplemental
IX	MSC-synthesized	8 Weeks	MSC	Supplemental
X	Collagen	N/A	MSC	Supplemental
XI	AFS-synthesized	4 Weeks	HEK	Osteogenic
XII	AFS-synthesized	8 Weeks	HEK	Osteogenic
XIII	MSC-synthesized	4 Weeks	HEK	Osteogenic
XIV	MSC-synthesized	8 Weeks	HEK	Osteogenic
XV	Collagen	N/A	HEK	Osteogenic

## **Statistical Analysis**

All statistical analysis was performed using GraphPad Prism (GraphPad Software, La Jolla, CA). For comparison between experimental groups and time points, an analysis of variance was performed with Tukey post hoc analysis. Differences were considered statistically significant if  $p < 0.05$ .

## **Results**

### **Decellularization**

The effectiveness of the decellularization process was evaluated via DNA quantification assays and live/dead staining. Figure 2.3 displays the results of the DNA quantification assay. The decellularization process reduced the quantity of DNA within the scaffold to less than 10% of the amount prior to decellularization. Images of the live/dead stained scaffolds were taken both pre (Figure 2.4.A-D) and post decellularization (Figure 2.4.E-H). Prior to decellularization, extensive numbers of live (green) cells were seen attached throughout the scaffold, while very few dead (red) cells were present. After the decellularization process virtually all cells within the scaffold were dead. Additional images were taken of a decellularized scaffold reseeded with MSCs (Figure 2.4.I-L). In addition to the dead cells left over from the decellularization process, significant numbers of live cells were seen repopulating all regions of the construct.

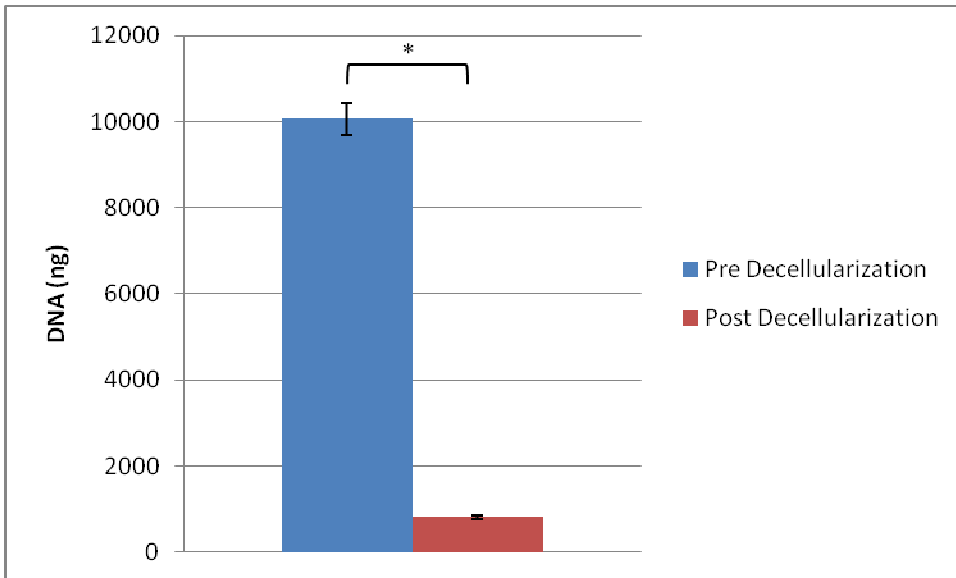


Figure 2.3: DNA content of scaffolds pre and post decellularization. Decellularization process significantly decreased cellularity of the scaffolds (n=4). \*  $p < 0.0001$ , error bars are  $\pm$  standard error.

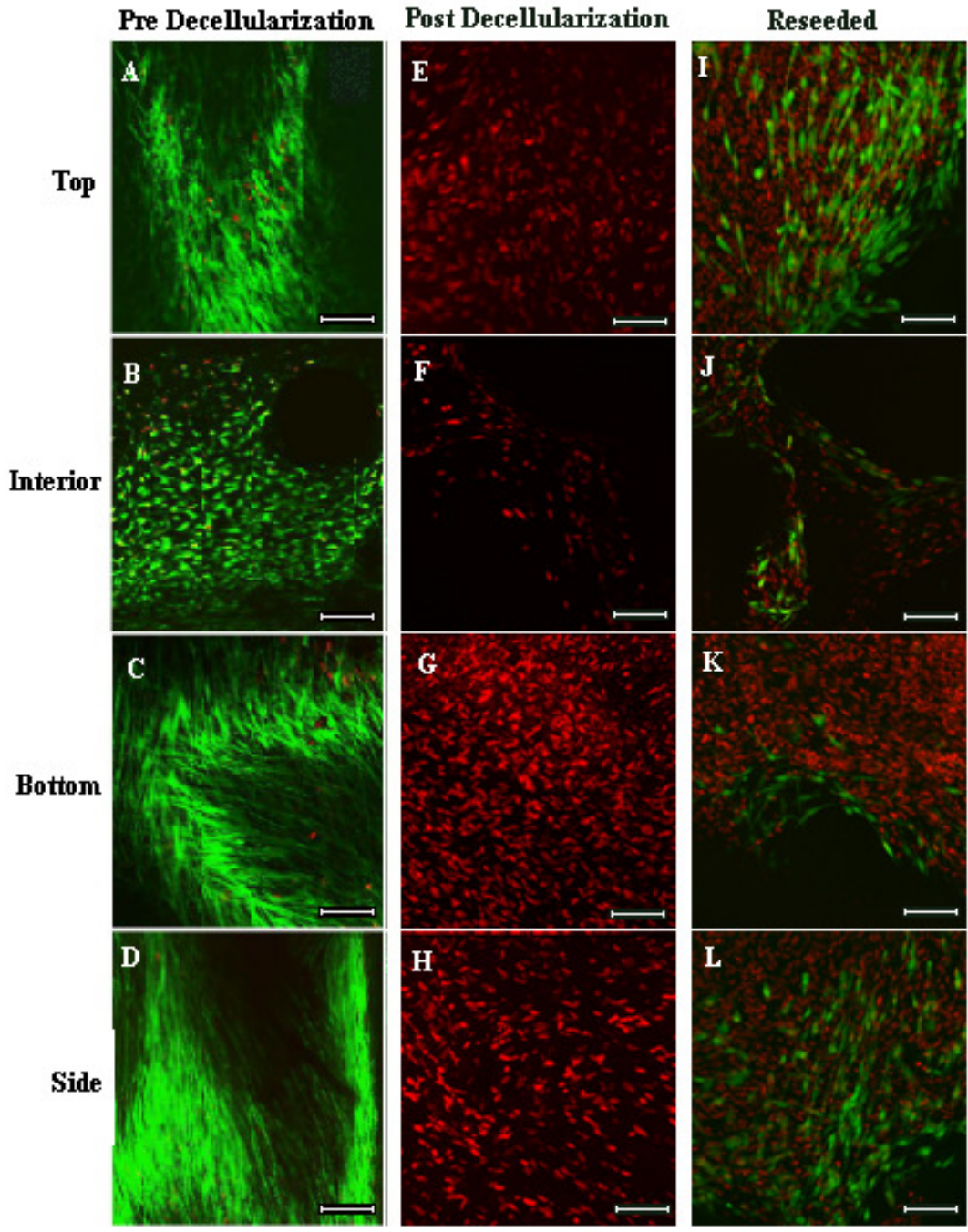


Figure 2.4: Confocal microscopy images of scaffolds pre decellularization (A-D), post decellularization (E-H), and reseeded with MSCs after decellularization (I-L). Live cells appear green and dead cells appear red. Images were taken of the exterior of the scaffolds at the top (A,E,I), bottom (C,G,K), and side (D,H,L), as well as of the interior by cutting the scaffold longitudinally (B,F,J). Scale bars are 100  $\mu$ m.

## 2D Studies

Results from the DNA quantification of MSCs cultured on 2D ECM can be seen in Figure 2.5. Cells were able to attach to and proliferate on ECM synthesized by both cell types. By 1 week there was an approximately 5 fold increase in the quantity of DNA present in the groups that had been reseeded with MSCs. This value held steady through two weeks and then decreased by week 3. At the time of reseeding and at 1 week, there was a significant difference between the DNA content of the AFS cell synthesized ECM that had been reseeded and MSC synthesized ECM that had been reseeded. However, there was also initially a significant difference between the acellular control groups. The initial difference between the reseeded MSC and AFS cell ECMs may therefore be due to differing initial amounts of DNA left over from the decellularization process. In fact, at the time of reseeding the difference in DNA quantity between the reseeded and acellular AFS ECM groups was about equal to the difference between the reseeded and acellular MSC ECM groups, and approximately equivalent to the 20,000 cells that had been reseeded. However, by the 3 week time point the DNA quantity in the reseeded AFS ECM group had decreased further than that of the reseeded MSC ECM group. Both acellular control groups contained a significant amount of DNA at the beginning of the culture period. This was most likely due to DNA that was left over from the decellularization process, as the values quickly subsided to near zero by week 1 as the left over DNA diffused out of the ECM.

The alkaline phosphatase activity of the MSCs cultured on each ECM type can be seen in Figure 2.6. In osteogenic media, the MSCs cultured on MSC ECM showed a peak in alkaline phosphatase activity at 1 week, followed by a decline. In contrast, MSCs

cultured on tissue culture plastic showed a gradual increase in alkaline phosphatase activity through 3 weeks. The value of alkaline phosphatase activity at the peak for the MSC ECM group was higher than any value reached by the group seeded on tissue culture plastic. The alkaline phosphatase activity of the MSCs seeded on AFS ECM never reached a value above the background level. Similar results were observed for cells cultured in the supplemental media. When comparisons were made between MSCs cultured on MSC ECM in osteogenic versus supplemental media, it was found that at weeks 0, 2, and 3 there was no significant difference. However, at the peak expression at 1 week the osteogenic group showed greater activity. Activity of the HEK cell control groups remained at the background level throughout the culture period.

Results of the calcium assay can be seen in Figures 2.7 and 2.8. The data is normalized by the initial amount of calcium from the preculture period to display only the calcium produced after reseeding. Figure 2.7 makes comparisons between the MSCs in osteogenic media, MSCs in supplemental media, and HEK cells for each ECM type. For the cells seeded on the AFS ECM, the MSCs in osteogenic media contained more calcium than the HEK cell group at 2 weeks, while the supplemental group did not reach a difference until 3 weeks. For the MSC ECM groups, the MSCs cultured in both osteogenic and supplemental media showed greater calcium content than the HEK cell group from week 1 onward. For cells cultured on tissue culture plastic, the calcium content for the osteogenic media group reached significance at 3 weeks, while the supplemental group did not reach a level of significance within the time period of this study.

Figure 2.8 uses the same data to make comparisons between the various matrix groups for the same media conditions. In osteogenic media, the MSC ECM group shows a difference compared to the no ECM group at 1 week, while the AFS ECM group does not show a difference until 2 weeks. However, there was no difference between the AFS ECM group and the MSC ECM group at any time with osteogenic media. In supplemental media, both AFS ECM and MSC ECM groups showed a difference compared to the no ECM group by 2 weeks. Additionally, the MSC ECM group had a higher calcium content than the AFS ECM group at this time, although this difference subsided by 3 weeks.



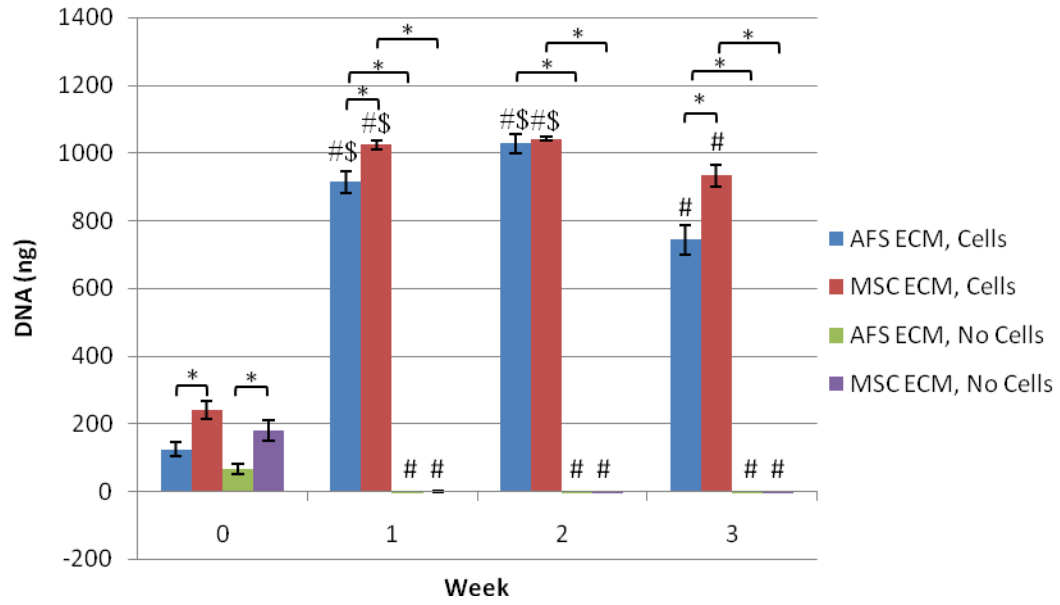


Figure 2.5: DNA quantification of MSCs cultured on AFS cell or MSC synthesized matrix.(n=6). \* p<0.05, # p<0.05 compared to week 0, \$ p<0.05 compared to week 3. Error bars are  $\pm$  standard error.

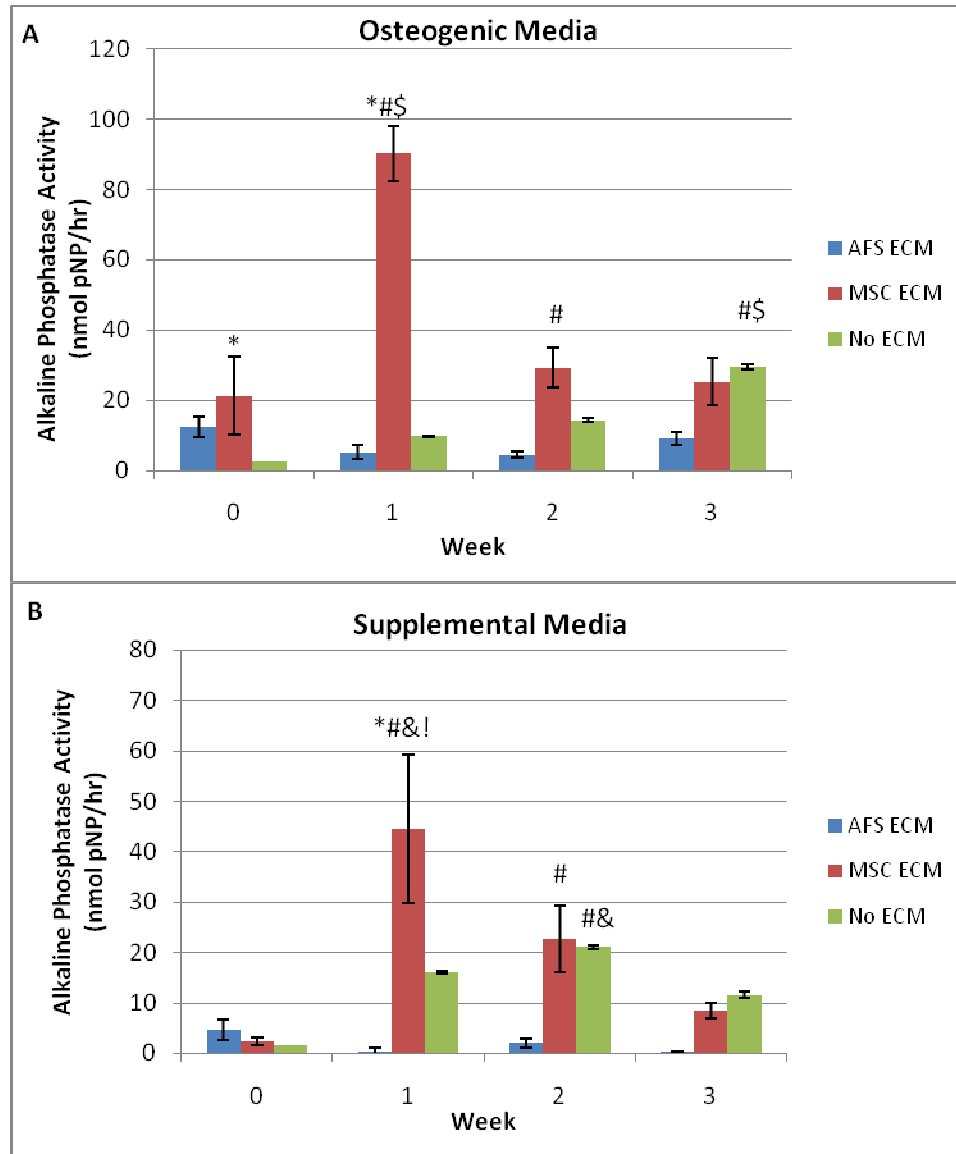


Figure 2.6: Alkaline phosphatase activity for MSCs cultured on ECM in A) osteogenic media, B) supplemental (n=6). \* p<0.05 compared to MSCs on tissue culture plastic, # p<0.05 compared to MSCs on AFS cell synthesized ECM, \$ p<0.05 compared to other time points, & p<0.05 compared to week 1, ! p<0.05 compared to week 3. Error bars are  $\pm$  standard error.

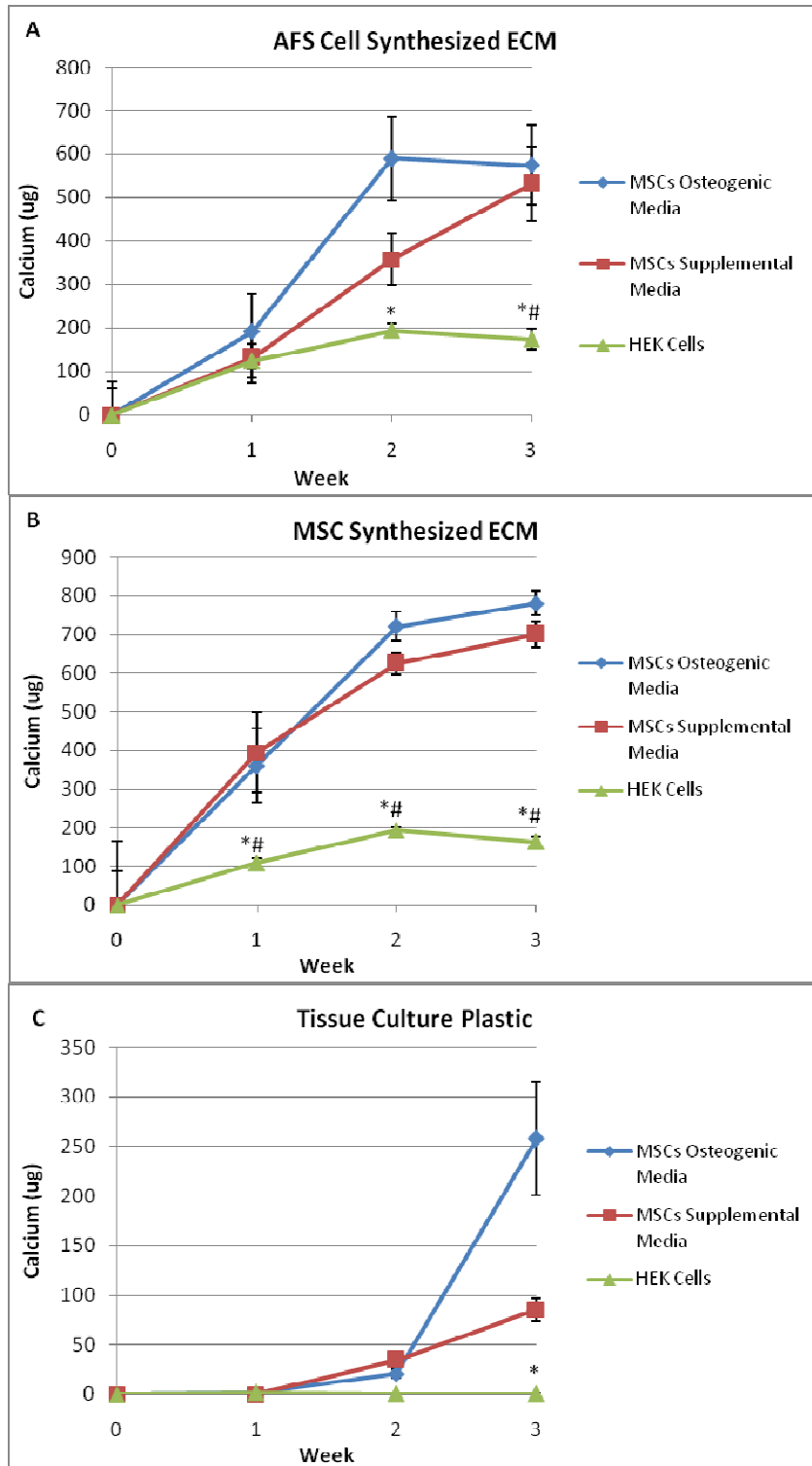


Figure 2.7: Calcium content for cells cultured on A) AFS cell synthesized ECM, B) MSC synthesized ECM, C) tissue culture plastic (n=6). \* p<0.05 compared to MSCs in osteogenic media, # p<0.05 compared to MSCs in supplemental media. Error bars are  $\pm$  standard error.

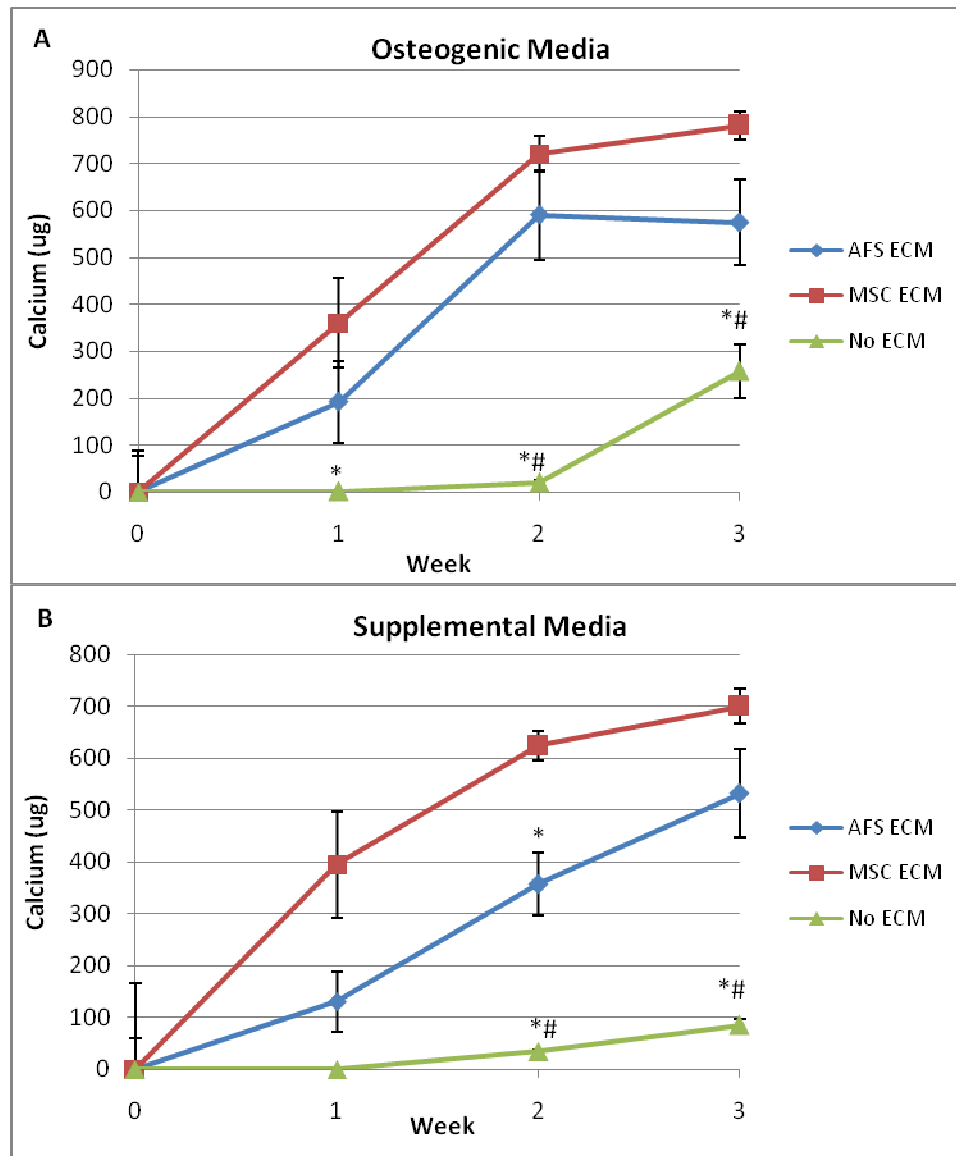


Figure 2.8: Calcium content for MSCs cultured on ECM in A) osteogenic media, B) supplemental (n=6). \* p<0.05 compared to MSCs on MSC synthesized ECM, # p<0.05 compared to MSCs on AFS cell synthesized ECM. Error bars are  $\pm$  standard error.

### 3D Studies

The 3D mineralization data is displayed in Figures 2.9-12. The data is normalized by the initial mineral volume produced during preculture to represent only the mineralization formed post-reseeding. Figures 2.9-11 compare mineral volume amounts between MSCs in osteogenic and supplemental media and HEK cells cultured on each ECM type and preculture time (4 and 8 weeks). For the MSC synthesized ECM, with both preculture periods the osteogenic group contained more mineralized matrix than the HEK cell group. Additionally on 4 week precultured ECM the osteogenic group also showed greater volume than the supplemental group. For the AFS ECM, with both preculture periods the osteogenic and supplemental groups both contained more mineral than the HEK cell group at 4 weeks. At 8 weeks, the osteogenic media group with 4 week precultured ECM also showed a greater amount than the corresponding supplemental media group. For cells cultured on collagen coated scaffolds, at 8 weeks the supplemental group was greater than the HEK cell group, while the osteogenic group was greater than both the HEK cell group and the supplemental group.

Figure 2.12 uses the same data to makes comparisons between the various matrix types and preculture periods. In osteogenic media, at 4 weeks both AFS ECM groups had greater mineralized matrix content than the MSC ECM or collagen groups. Additionally, at this time the 8 week preculture AFS group had a greater volume of mineral than the 4 week preculture AFS group. By 8 weeks, both MSC groups caught up to the 4 week preculture AFS group. Both the 4 week preculture groups were greater than the collagen group. The 8 week preculture AFS group remained greater than all other groups at this time. For the supplemental media, the differences observed were the same

as with the osteogenic media at the same time point. However, at 8 weeks, while the 8 week preculture AFS group remained greater than all other groups, the 4 week preculture AFS group was greater than the 4 week preculture MSC group and collagen group, and there is no difference between the collagen group and either MSC group. Figures 2.13 and 2.14 show representative microCT images of each group at the 4 and 8 week time points respectively.

From the DNA quantification assay, it was found that the attachment efficiency for reseeded MSCs differed between the ECM groups and the collagen scaffolds (Figure 2.15). While approximately 95% of the 2 million cells that were reseeded onto the collagen scaffolds attached, only about 25 to 50% of the cells reseeded on the various ECM types attached. However, the number of cells on each scaffold increased significantly during the first week of culture, and by 1 week there was no difference in the DNA quantity between any of the ECM groups or the collagen scaffolds (Figure 2.16).

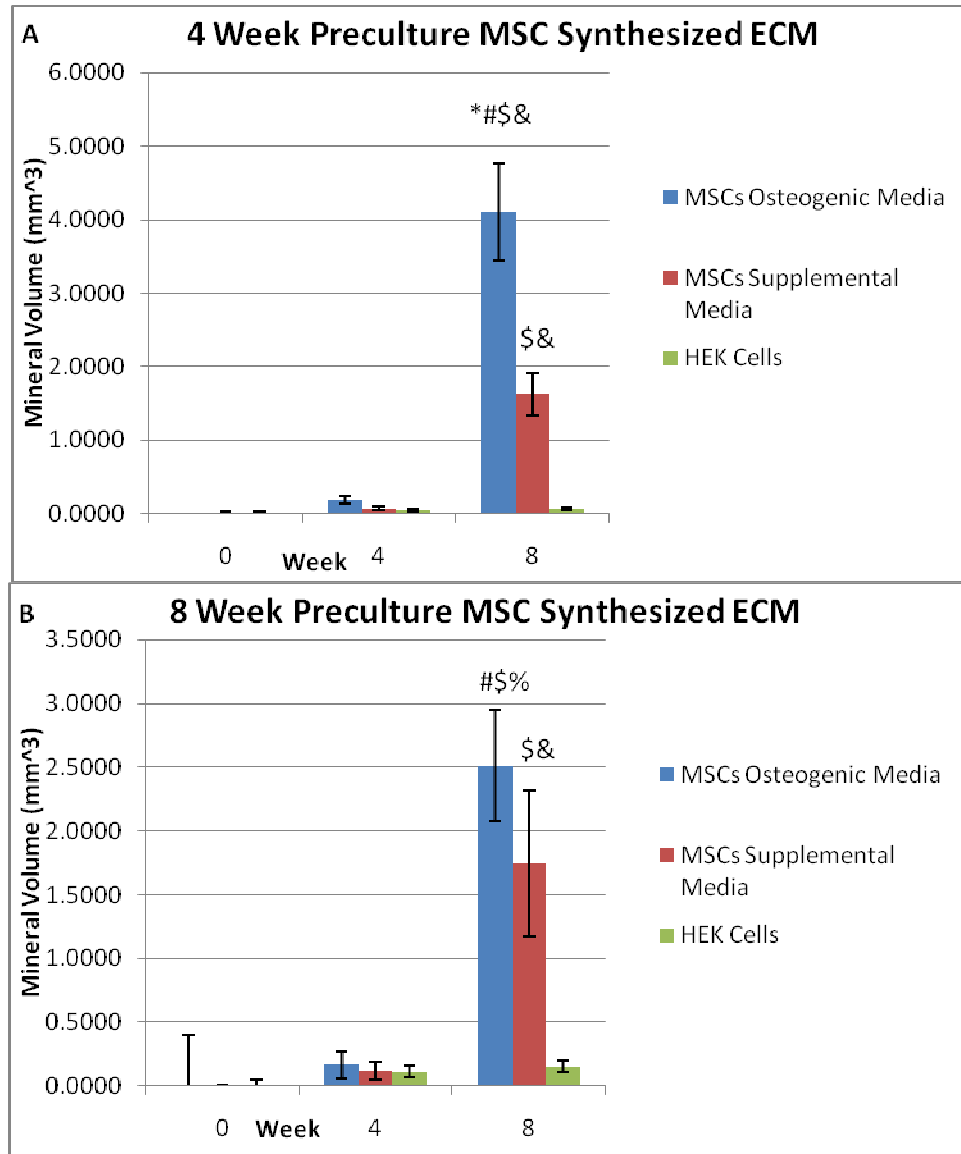


Figure 2.9: 3D mineralized matrix volume produced by cells cultured on MSC synthesized ECM with preculture periods of A) 4 weeks B) 8 weeks (n=6). \* p<0.05 compared to supplemental media, # p<0.05 compared to HEK cells, \$ p<0.05 compared to week 0, & p<0.05 compared to week 4. Error bars are  $\pm$  standard error.

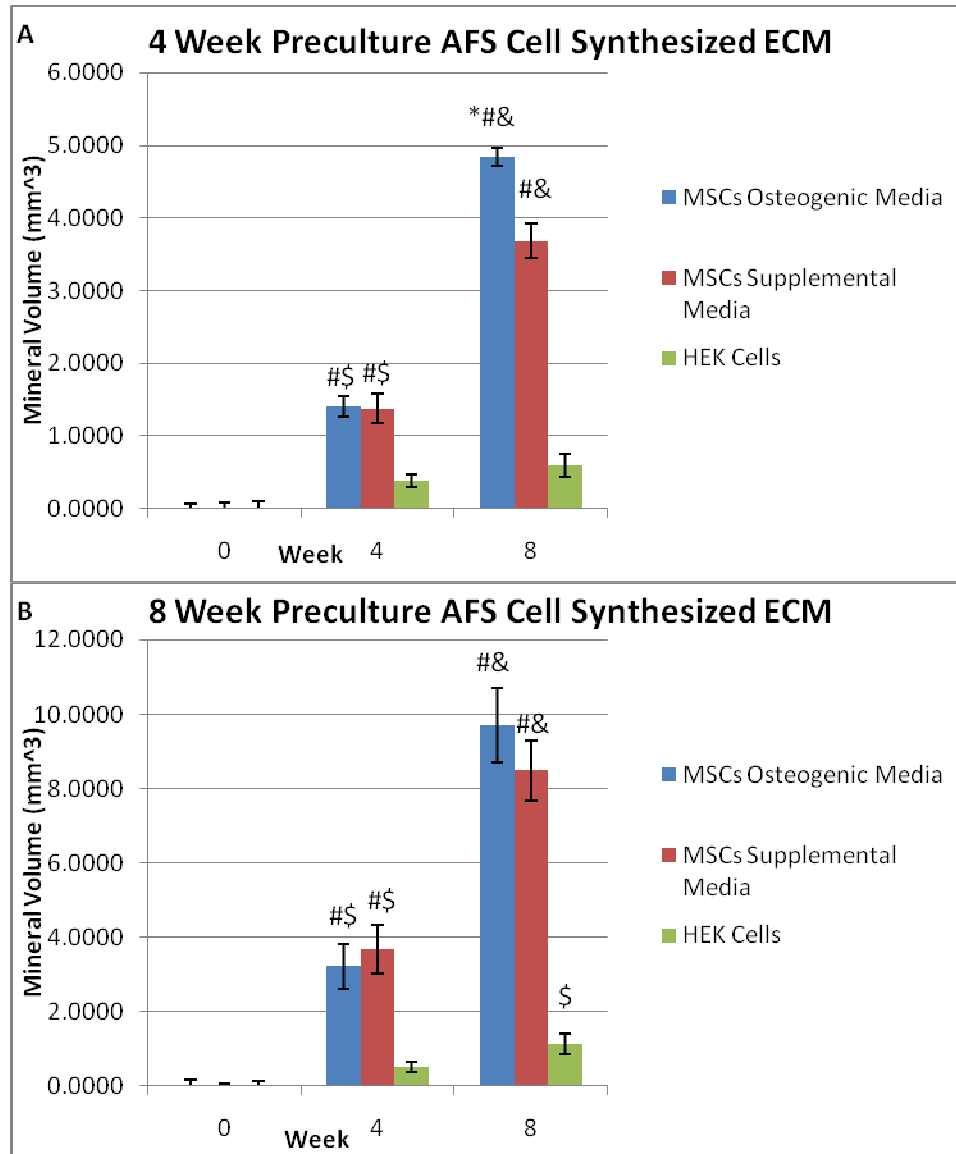


Figure 2.10: 3D mineralized matrix volume produced by cells cultured on AFS cell synthesized ECM with preculture periods of A) 4 weeks B) 8 weeks (n=6). \* p<0.05 compared to supplemental media, # p<0.05 compared to HEK cells, \$ p<0.05 compared to week 0, & p<0.05 compared to week 4. Error bars are  $\pm$  standard error.



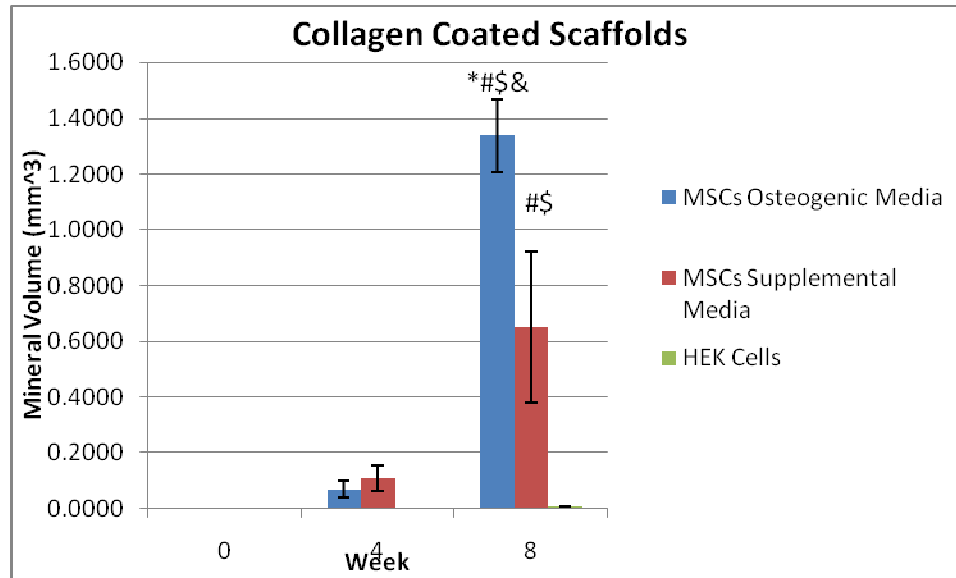


Figure 2.11: 3D mineralized matrix volume produced by cells cultured on collagen coated scaffolds (n=6). \*  $p < 0.05$  compared to supplemental media, #  $p < 0.05$  compared to HEK cells, \$  $p < 0.05$  compared to week 0, &  $p < 0.05$  compared to week 4. Error bars are  $\pm$  standard error.

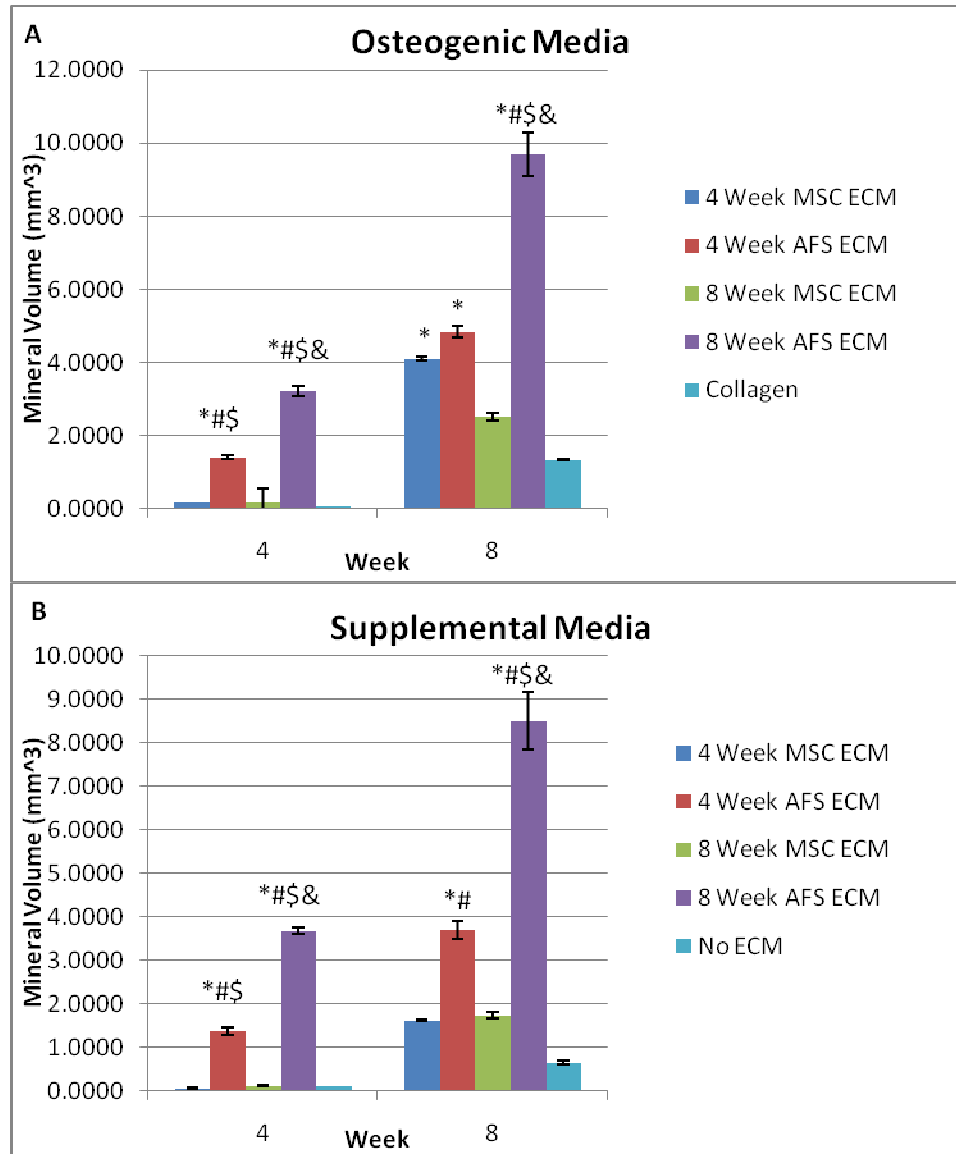


Figure 2.12: 3D mineralized matrix volume produced by MSCs cultured in A) osteogenic media B) supplemental media (n=6). \* p<0.05 compared to collagen coated scaffolds, # p<0.05 compared 4 week precultured MSC synthesized ECM, \$ p<0.05 compared to 8 week precultured MSC synthesized ECM, & p<0.05 compared to 4 week precultured AFS cell synthesized ECM. Error bars are  $\pm$  standard error.

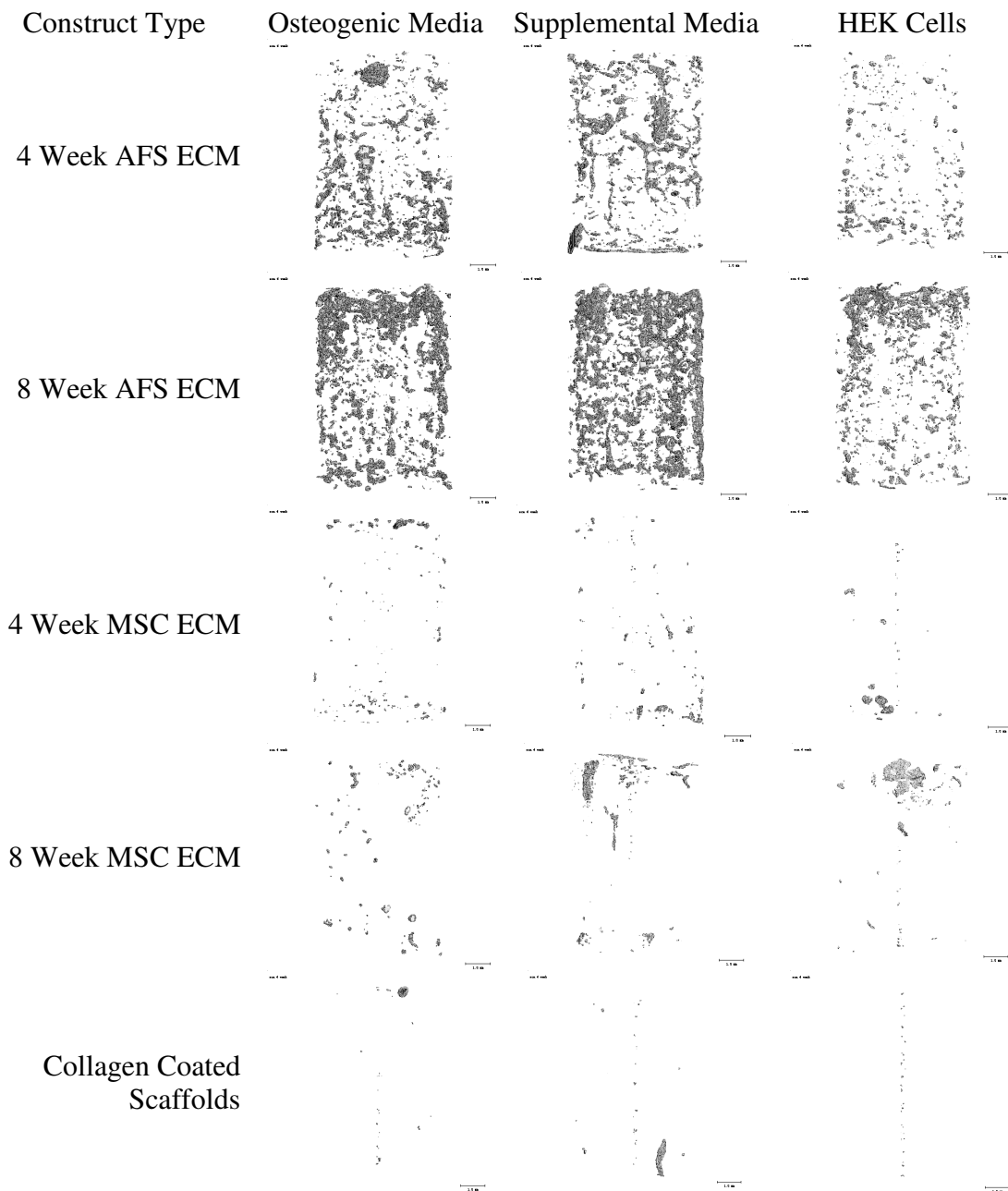


Figure 2.13: MicroCT images of 3D constructs 4 weeks following reseeding. Images are representative of the average value of mineral volume for each group at the 4 week time point. The columns show in order: reseeded MSCs cultured in osteogenic media, reseeded MSCs cultured in supplemental media, and reseeded HEK cells cultured in osteogenic media. Scale bars are 1 mm.

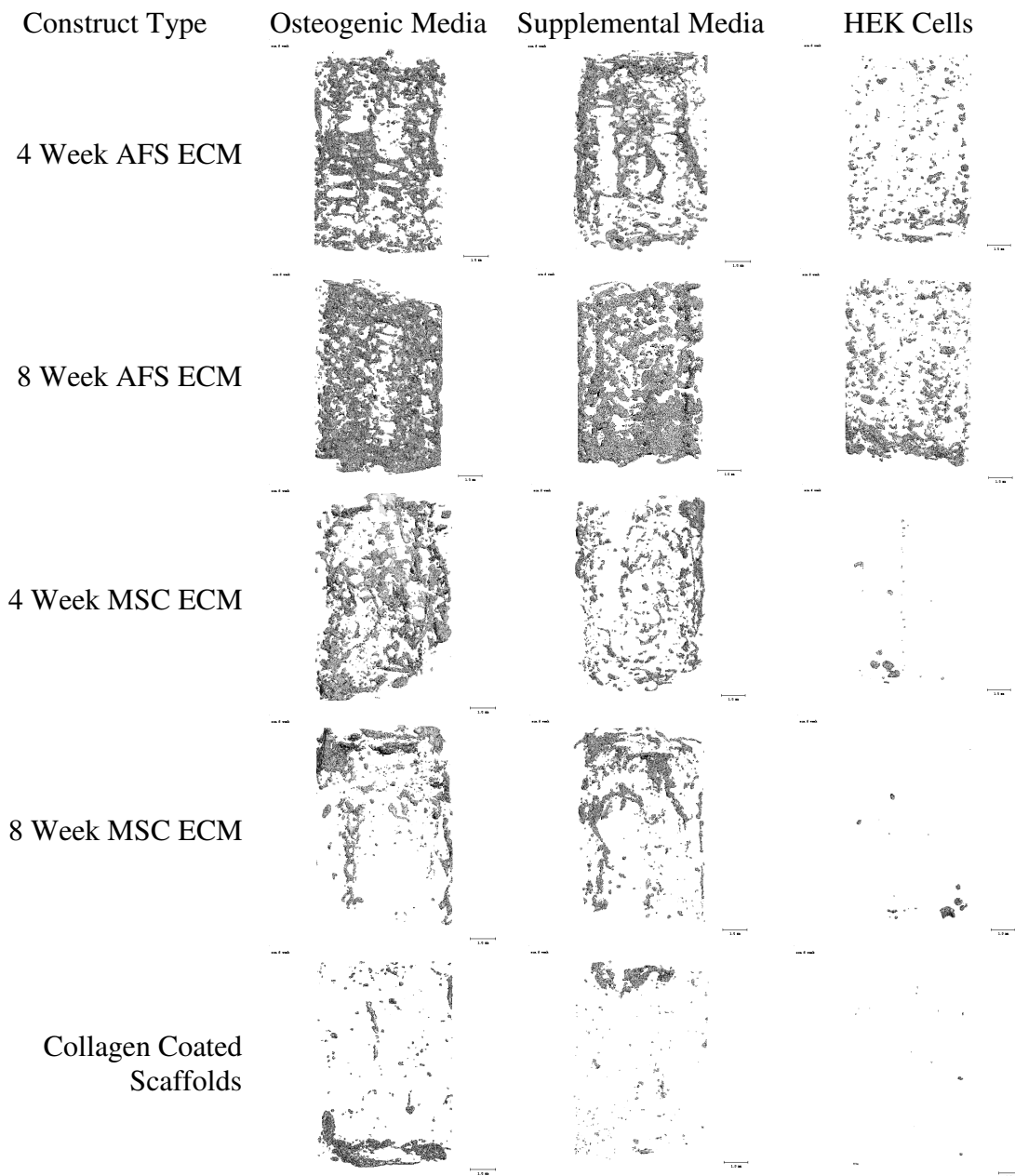


Figure 2.14: MicroCT images of 3D constructs 8 weeks following reseeding. Images are representative of the average value of mineral volume for each group at the 8 week time point. The columns show in order: reseeded MSCs cultured in osteogenic media, reseeded MSCs cultured in supplemental media, and reseeded HEK cells cultured in osteogenic media. Scale bars are 1 mm.

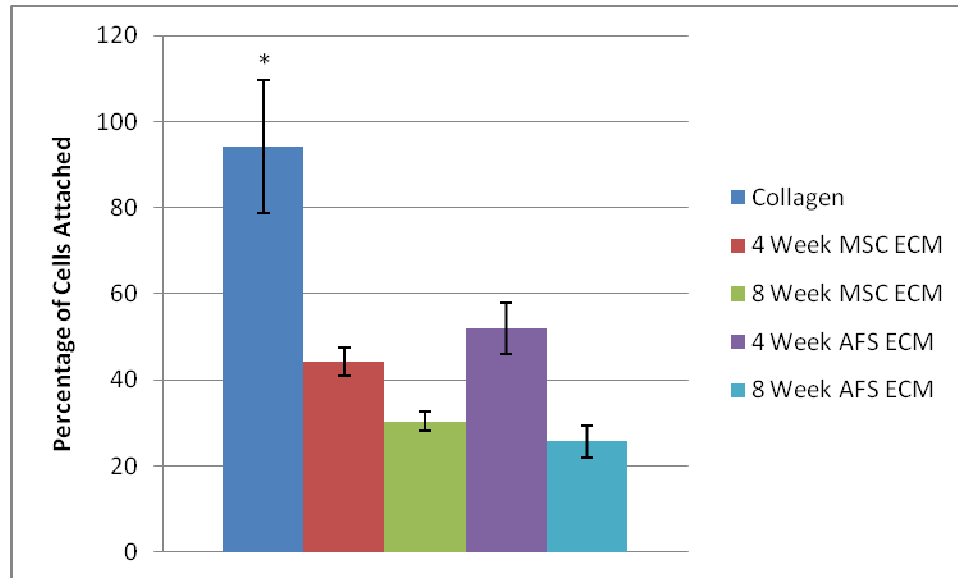


Figure 2.15: Cell attachment proficiency for MSCs reseeded onto decellularized ECM (n=4). \*  $p < 0.05$  compared to cell synthesized ECM groups. Error bars are  $\pm$  standard error.

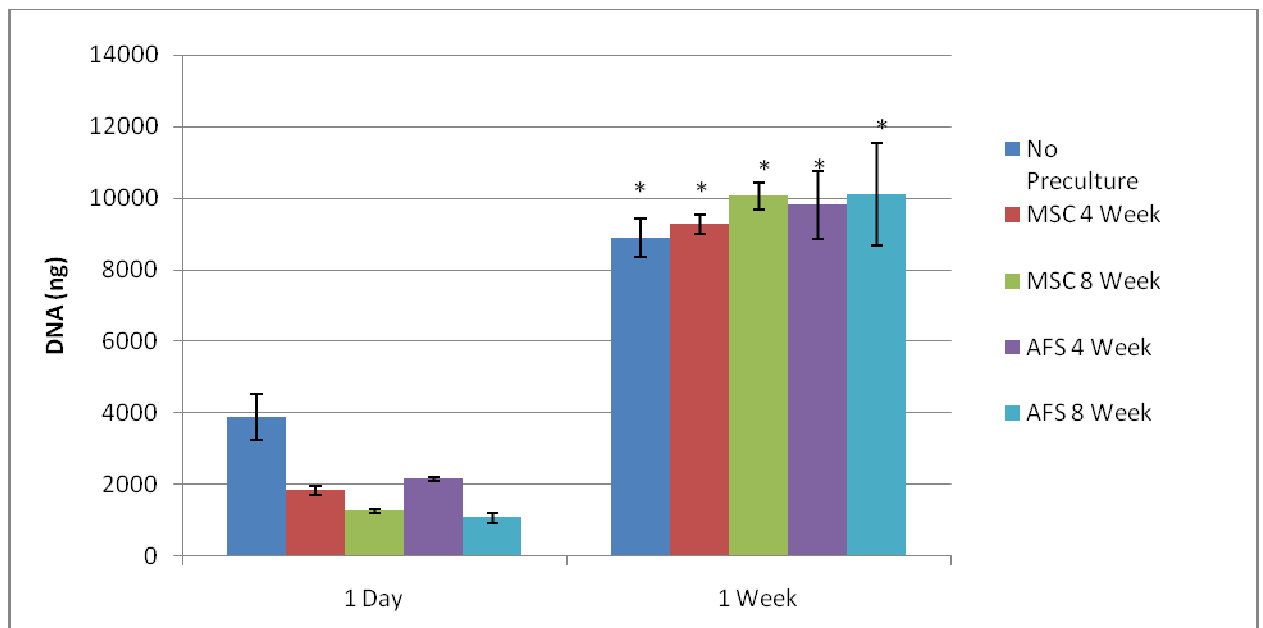


Figure 2.16: DNA content of decellularized ECM constructs 1 day and 1 week following reseeding with MSCs (n=4). \*  $p < 0.05$  compared to day 1. Error bars are  $\pm$  standard error.

## Discussion

This aim set out to use *in vitro* analysis techniques to characterize stem cell synthesized ECM for use in bone tissue engineering applications. The success of these studies depended foremost on the effectiveness of the decellularization procedure and the ability of the MSCs to repopulate the acellular ECM. The DNA quantification data displays that the decellularization process was successful in devitalizing most, if not all of the cells within the ECM. In 2D without reseeded cells, the quantity of DNA quickly went to zero by one week in culture as DNA entrapped within the matrix left over from decellularization diffused out. In 3D, the decellularization process removed over 90% of the DNA from the ECM. Even the small amount of DNA left over was most likely not associated with live cells, but rather free DNA entrapped within the matrix similar to the 2D study. The conclusions were further confirmed by the live/dead staining. Although the scaffolds were saturated with live cells before decellularization, after freeze/thawing and treatment with DNase virtually none could be found in any region of the scaffold.

Not only was the decellularization process successful, but results also showed that MSCs were able to repopulate and proliferate on the acellular ECM. Live/dead staining of reseeded scaffolds showed live MSCs throughout the scaffold. The distribution of the cells on the scaffold was important because they were seeded from the top only. Their presence at the bottom and within the interior of the scaffold indicates that they were either able to diffuse through the pores within the scaffold or migrate along the surface of the ECM. Cells were able to proliferate on both AFS and MSC synthesized ECM. In both the 2D and 3D cultures, the DNA content increased approximately 5 fold after 1 week. In 2D this was a saturation point, with the cells maintaining that number for another week

before decreasing in DNA content at 3 weeks. For the 3D culture, the collagen coated scaffolds initially had a higher number of cells attach. However, the DNA content of these scaffolds at 1 week was approximately the same as the ECM coated scaffolds. Therefore, the cells actually proliferated less during the first week of culture on the collagen than on the various ECM types. However, from this data it could not be determined whether the ECM had a greater proliferative effect on the cells, or if the cells were hitting a saturation point on the scaffolds by the 1 week time point.

Previous work has been done to evaluate the osteoinductivity of MSC-synthesized ECM.[9, 19, 20, 21, 22] It was observed that culturing MSCs on the MSC-synthesized ECM resulted in increased alkaline phosphatase activity and calcium content, indicative of osteogenic differentiation.[9] Similar results were observed in these studies. Additionally, a synergistic effect was previously observed when adding dexamethasone to the culture media for the cells cultured on the ECM.[9] This effect was also observed in the alkaline phosphatase activity data in these studies. The cells cultured in 2D on the AFS cell synthesized ECM did not perform as well as the MSC ECM cultured cells in these measures of osteogenic differentiation. Although the calcium content did increase for these cells in both the osteogenic and supplemental media, it was at a slower rate than the cells cultured on MSC ECM. Additionally, the AFS ECM groups did not show significant levels of alkaline phosphatase activity. These results suggest that with 3 weeks of 2D preculture, ECMs synthesized by both cell types have osteoinductive capabilities as indicated by the increased calcium content in comparison to cells cultured on tissue culture plastic. Additionally, MSC synthesized ECM acts as a better osteoinductive agent than AFS cell synthesized ECM, as measured by the alkaline phosphatase activity.

In 3D the opposite effect was observed. At each time point, preculture period, or media condition, the cells cultured on the AFS cell synthesized matrix either matched or exceeded the cells cultured on MSC synthesized matrix in terms of volume of mineral produced. Within the AFS ECM groups, the 8 week preculture period resulted in the reseeded cells producing more mineralized matrix than their 4 week preculture counterparts. The difference in mineral volume between the 8 week preculture AFS ECM and MSC ECM was greater than the difference between the 4 week preculture groups. These results suggest that in 3D with preculture periods of 4 weeks or longer, AFS cell synthesized ECM induce more mineralized matrix formation than MSC synthesized ECM, and that longer preculture periods result in a greater effect, at least up until 8 weeks.

In the 2D studies, the MSC synthesized ECM had a greater osteoinductive effect on reseeded MSCs. However, in the 3D studies, the AFS cell synthesized ECM induced greater mineralized matrix production. One possible explanation for this discrepancy may be a difference between 2D and 3D culture. The ECM may induce osteogenic differentiation by altering the micro-environment of the cells. If the micro-environment is different between 2D versus 3D culture, this may account for the different effects on the cells. If this is the case, the AFS cell synthesized ECM would make the more likely candidate for a bone tissue engineering therapy, as bone repair takes place in a 3D environment and the AFS ECM performed better in 3D.

A second explanation for the different effects seen could be related to the preculture period. With the shorter preculture period the MSC ECM showed greater osteoinductivity. However, with a longer preculture period the AFS ECM induced greater



mineralized matrix production. This difference may be related to the initial maturity level of the cells. The MSCs are initially a more differentiated cell type. Because of this, with shorter preculture times the MSCs become further differentiated and the ECM is more specific towards the osteogenic lineage compared to the AFS ECM. However, with more preculture, the AFS have more time to differentiate and the ECM they produce becomes more mature. This may cause the ECMs effect on the mineralized matrix production of reseeded cells to become more pronounced. If this is the case, AFS cell ECM precultured for a longer period of time would be more ideal for a bone tissue engineering therapy.

In this aim, the decellularization procedure of freeze/thaw cycling followed by DNase treatment was found to successfully decellularize the stem cell synthesized extracellular matrix. MSCs were able to then repopulate and proliferate on this matrix. In 2D, ECM that was synthesized by MSCs had a greater osteoinductive effect on reseeded MSCs. However, in 3D, AFS cell synthesized matrix proved to cause greater mineralized matrix production, with a longer preculture period resulting in a greater effect.

## References

1. Siffert RS. *The role of alkaline phosphatase in osteogenesis*. J Exp Med, 1951. 93(5): 415-426.
2. Jaiswal N, Haynesworth SE, Caplan AI, Bruder SP. *Osteogenic differentiation of purified, culture-expanded human mesenchymal stem cells in vitro*. J Cell Biochem, 1997. 64(2): 295-312.
3. Hutmacher DW, Schantz JT, Lam CX, Tan KC, Lim TC. *State of the art and future directions of scaffold-based bone engineering from a biomaterials perspective*. J Tissue Eng Regen Med, 2007. 1(4): 245-260.
4. Zein I, Hutmacher DW, Tan KC, Teoh SH. *Fused deposition modeling of novel scaffold architectures for tissue engineering applications*. Biomaterials, 2002. 23(4): 1169-1185.
5. Porter BD, Lin AS, Peister A, Hutmacher D, Guldberg RE. *Noninvasive image analysis of 3D construct mineralization in a perfusion bioreactor*. Biomaterials, 2007. 28(15): 2525-2533.
6. Lan CW, Wang FF, Wang YJ. *Osteogenic enrichment of bone-marrow stromal cells with the use of flow chamber and type I collagen-coated surface*. J Biomed Mater Res A, 2003. 66(1): 59-68.
7. Cartmell S, Huynh K, Lin A, Nagaraja S, Guldberg R. *Quantitative microcomputed tomography analysis of mineralization within three-dimensional scaffolds in vitro*. J Biomed Mater Res A, 2004. 69(1): 97-104.
8. Guldberg RE, Duvall CL, Peister A, Oest ME, Lin AS, Palmer AW, Levenston ME. *3D imaging of tissue integration with porous biomaterials*. Biomaterials, 2008. 29(28)L 3757-3761.
9. Datta N, Holtorf HL, Sikavitsas VI, Jansen JA, Mikos AG. *Effect of bone extracellular matrix synthesized in vitro on the osteoblastic differentiation of marrow stromal cells*. Biomaterials, 2005. 26(9): 971-977.
10. Nair R, Ngangan AV, McDevitt TC. *Efficacy of solvent extraction methods for acellularization of embryoid bodies*. J Biomater Sci Polym Ed, 2008. 19(6): 801-819.
11. Ngangan AV, McDevitt TC. *Acellularization of embryoid bodies via physical disruption methods*. Biomaterials, 2009. 30(6): 1143-1149.
12. DeCoppi P, Bartsch G Jr, Siddiqui MM, Xu T, Santos CC, Perin L, Mostoslavsky G,

- Serre AC, Snyder EY, Yoo JJ, Furth ME, Soker S, Atala A. *Isolation of amniotic stem cell lines with potential for therapy*. Nat Biotechnol, 2007. 25(1): 100-106.
13. Prockop DJ. *Marrow stromal cells as stem cells for nonhematopoietic tissues*. Science, 1997. 276(5309): 71-74.
  14. Colter DC, Class R, DiGirolamo CM, Prockop DJ. *Rapid expansion of recycling stem cells in cultures of plastic-adherent cells from human bone marrow*. Proc Natl Acad Sci USA, 2000. 97(7): 3213-3218.
  15. Peister A, Deutsch ER, Kolambkar Y, Hutmacher DW, Guldberg R. *Amniotic fluid stem cells produce robust mineral deposits on biodegradable scaffolds*. Tissue Eng Part A, 2009. [Epub ahead of print]
  16. Peister A, Mellad JA, Larson BL, Hall BM, Gibson LF, Prockop DJ. *Adult stem cells form bone marrow (MSCs) isolated from different strains of inbred mice vary in surface epitopes, rates of proliferation, and differentiation potential*. Blood, 2004. 103(5): 1662-1668.
  17. Tremoleda JL, Forsyth NR, Khan NS, Wojtacha D, Christodoulou I, Tye BJ, Racey SN, Collishaw S, Sottile V, Thomson AJ, Simpson AH, Noble BS, McWhir J. *Bone tissue formation from human embryonic stem cells in vivo*. Cloning Stem Cells, 2008. 10(1): 119-132.
  18. Cartmell SH, Porter BD, Garcia AJ, Guldberg RE. *Effects of medium perfusion rate on cell-seeded three-dimensional bone constructs in vitro*. Tissue Eng, 2003. 9(6): 1197-1203.
  19. Datta N, Pham QP, Sharma U, Sikavitsas VI, Jansen JA, Mikos AG. *In vitro generated extracellular matrix and fluid sheer stress synergistically enhance 3D osteoblastic differentiation*. Proc Natl Acad Sci USA, 2006. 103(8): 2488-2493.
  20. Pham QP, Kasper FK, Mistry AS, Sharma U, Yasko AW, Jansen JA, Mikos AG. *Analysis of the osteoinductive capacity and the angiogenicity of an in vitro generated extracellular matrix*. J Biomed Mater Res A, 2009. 88(2): 295-303.
  21. Pham QP, Kasper FK, Scott Baggett L, Raphael RM, Jansen JA, Mikos AG. *The influence of an in vitro generated bone like extracellular matrix on osteoblastic gene expression of marrow stromal cells*. Biomaterials, 2008. 29(18): 2729-2739.
  22. Sikavitsas VI, van den Dolder J, Bancroft GN, Jansen JA, Mikos AG. *Influence of the in vitro culture period on the in vivo performance of cell/titanium bone tissue-engineered constructs using a rat cranial critical size defect model*. J Biomed Mater Res A, 2003. 67(3): 944-951.

## CHAPTER 3

# ***IN VIVO* EVALUATION OF THE BONE REGENERATIVE POTENTIAL OF STEM CELL SYNTHESIZED EXTRACELLULAR MATRIX**

### **Introduction**

*In vitro* studies provide an efficient, cost-effective method of characterizing a potential therapy. However, short of clinical trials in humans, the best way to evaluate the true usefulness of a therapy is through *in vivo* animal models. There are a complex array of factors that influence an engineered construct at the site of tissue repair. These include mechanical and chemical stimuli, migrating cells, angiogenesis, mass transport limitations, and immune responses. While *in vitro* experiments may be designed that mimic some of these factors, it is the culmination of all of these components that controls the healing response induced by the therapeutic agent. While the anatomy and physiology of other animals differs from that of humans, animal models still provide a much closer approximation of the clinically relevant environment than even the most complex of *in vitro* models can come close to achieving. Because of this, animal studies are considered the ultimate preclinical test for any emerging therapy.

Several animal models exist for the evaluation of potential bone tissue engineering therapies. The simplest of these models is the ectopic model, which involves implanting the construct within the subcutaneous space.[1] This model is useful for showing osteoinduction by the potential therapeutic agent, as there are no native osteoinductive factors at the implantation site. Additionally, it is efficient as it allows several groups to be compared within each animal. However, this model is not directly

clinically relevant as it does not involve the healing of a bone defect. The calvarial defect model involves creating a defect within the top of the skull. These defects have the advantages of being easy to create and requiring no fixation device.[2] However, this model is limited by a high rate of spontaneous healing due to the high vascularity of the region, as well as the presence of an excellent source of osteoprogenitor cells within the surrounding periosteum and cranial bone marrow. A more challenging model is preferred to allow for better discernment between groups. Long bone defects have been created in the radius, ulna, tibia, and femur of several animal types, including mice, rats, rabbits, and dogs.[3] Rodent long bone defects have been used extensively in preclinical animals studies due to their short times to skeletal maturity, limited housing requirements, and low cost when compared to larger animals. Of the various long bone defect types, the femoral segmental defect provides perhaps the most challenging model due to its lack of proximity to other bones that may contribute vascularity or osteoprogenitor cells to the osteotomy.

In this study, an 8 mm rat femoral segmental defect model was used. Previous studies have utilized a 5 mm defect model to test potential therapies. However, with this smaller defect size, spontaneous healing was found to occur even without treatment.[4, 5] As a result, the more challenging 8 mm defect model was established.[6, 7] Spontaneous healing will not occur with this defect size, meeting the criteria of a critically sized defect.[8] Defects in this study were stabilized using a custom modular fixation plate made of polysulfone (Figure 3.1). The low radiopacity of these plates creates a window for x-ray and microCT scanning of the defect to noninvasively monitor and quantify healing over time.

The goal of this aim was to evaluate the bone regenerative potential of ECM produced by osteogenically induced AFS cells and compare it to that of MSCs. It was hypothesized that the mineralization and bridging of defects containing ECM constructs would be greater than that of the empty scaffolds.

## **Materials and Methods**

### **Scaffold Preparation**

Scaffolds were prepared in the same manner as the *in vitro* 3D studies. In brief, cylindrical scaffolds measuring 6 mm diameter by 9 mm thick were created from PCL sheets. Scaffolds were treated with 5 M NaOH to roughen the surface, sterilized via ethanol evaporation, and coated with lyophilized collagen to improve cell attachment.[9] Two million cells (either AFS cells or MSCs) were seeded on the scaffolds and cultured in osteogenic media for 8 weeks to produce ECM. The 8 week preculture time was chosen based on the *in vitro* studies, as this time showed the greatest mineralized matrix formation in 3D culture. After the preculture period, the scaffolds were decellularized via freeze/thaw cycling and DNase treatment and lyophilized to create greater porosity for cellular infiltration. Three groups were included in the *in vivo* study: AFS cell synthesized ECM, MSC synthesized ECM, and collagen coated scaffolds as a control (n=10)

### **Femoral Segmental Defect Surgery**

All animals studies were performed within the guidelines of protocol A06020 approved by the Institutional Animal Care and Use Committee at the Georgia Institute of Technology. All surgical procedures were performed under general anesthesia (Isoflourane) using aseptic techniques. Femoral segmental defects were created

bilaterally in 13 week old athymic female nude rats (Charles River Laboratories, Wilmington, MA) . Prior to the procedure, the incision site was shaved and scrubbed, alternating chlorhexidine with isopropyl alcohol. An incision was made over the anterior length of the femur. Blunt dissection of the quadriceps muscle along the muscle bundle lines was used to expose the femur. After all soft tissue had been cleaned away from the bone, a rigid fixation plate was attached to the anterolateral surface of the femur using two screws at each end (Figure 3.1). An 8 mm defect was then created in the diaphysis of the bone with an oscillating saw. Scaffolds were then wet with 300 mOsm/L saline solution and press fit into the defect site. Resorbable sutures and wound clips were used to close the incision site in two layers. Following recovery from anesthesia, animals were given subcutaneous buprenorphine injections every 8 hours for 72 hours for pain management. All animals recovered normal ambulation within 3 to 7 days following surgery. Wound clips were removed 14 days post-surgery.[6] Animals were housed in sterile housing, fed gamma-irradiated chow, and given sterile water.

### **X-Ray and MicroCT Analysis**

Healing of the bone defects was analyzed *in vivo* using both x-ray and microCT. Animals were anesthetized using Isoflurane during scanning. Each leg was scanned independently using a high resolution x-ray system (Faxitron X-Ray LLC, Lincolnshire, IL) at 4, 8, and 12 weeks. X-rays were used to determine whether the defects had bridged, defined by a continuous span of bone from one side of the defect to the other.[6]

Following x-ray scanning, each leg was also imaged using microCT at each time point (VivaCT scanner, Scanco Medical, Switzerland). All scans were performed at a 38  $\mu\text{m}$  voxel resolution. The scanning region was defined as the space between the metal

attachment plates at either end of the defect. Scans were used to quantify mineral formation within the defect site. For analysis, only the central region of the defect was used. To locate this region, 2D slices were examined to find the end of the native cortical bone at both the proximal and distal ends of the defect. From these points, the center point and corresponding slice was calculated. The analysis region included this slice as well as 62 slices in either direction (125 total slices). Although the defect was 8 mm in length, this region only corresponds to the middle 4.75 mm. This reduction in the analysis region is necessary because of the angled alignment of the femurs with the axis of scanning. Due to space constraints in the microCT system, it is not possible to align the axis of the femur perfectly with the axis of the scanner. Because only the quantity of new bone produced is desired, this angle decreases the assessable volume of interest (VOI) that excludes the native cortical bone (Figure 3.2). To determine the value used, each scan was examined to determine the effective distance between the native bone on either side of the defect at the angle the bone was scanned. The chosen value of 4.75 mm was the value of the scan that had the least distance between the ends of the native bone. That way, each scan could be evaluated with the same VOI without including native cortical bone. Scans were evaluated at a threshold of 100, a filter width of 1.2, and a filter support of 2 (n=10).[6, 11] At 12 weeks post surgery, animals were sacrificed and limbs were harvested.

### **Statistical Analysis**

All statistical analysis was performed using GraphPad Prism (GraphPad Software, La Jolla, CA). For comparison between experimental groups and time points, an analysis



of variance was performed with Tukey post hoc analysis. Differences were considered statistically significant if  $p < 0.05$ .

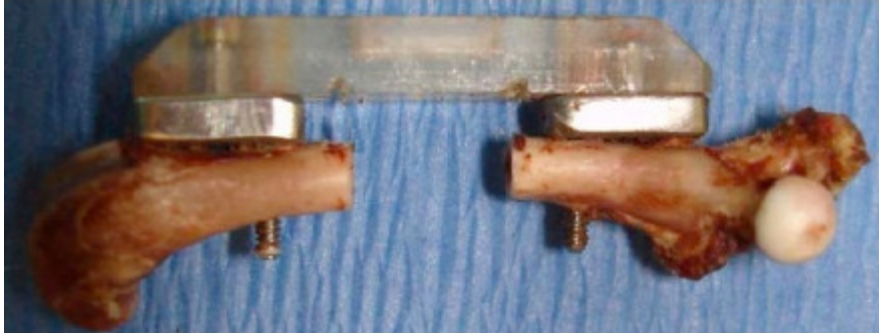


Figure 3.1: Femoral segmental defect with attached polysulfone fixation plate.

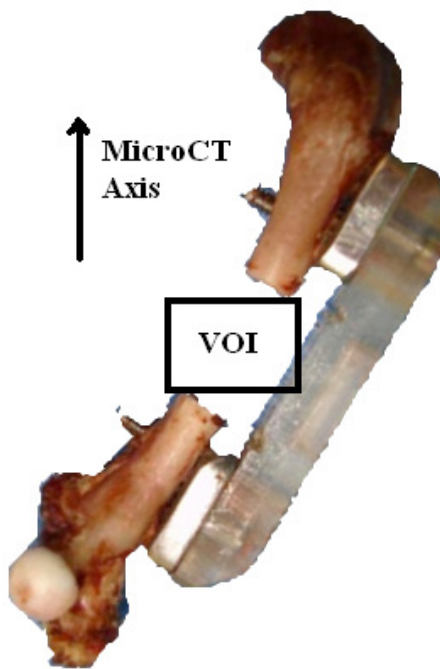


Figure 3.2: Volume of interest (VOI) used for microCT analysis of defect site.

## Results

One of the collagen scaffold treated limbs was omitted from evaluation due to fracturing of the femur around the screw holes at the proximal fixation site (n=9 for collagen group). Faxitron x-ray images were taken at 4, 8, and 12 weeks post surgery to monitor new bone formation. The resulting images for the AFS ECM, the MSC ECM, and the collagen coated scaffolds can be seen in Figure 3.3, 3.4, and 3.5 respectively. There was a lot of variance between the samples in each group, with some limbs showing little to no mineralization, while others showed significant amounts throughout the defect. The images were used to determine if the defects had bridged, defined by a continuous expanse of mineralized tissue from the proximal to distal end of the defect (Table 3.1). Based on this criterion, for the AFS synthesized ECM group, 2 defects had bridged at 4 weeks. However, only 1 additional defect bridged between 8 and 12 weeks, for a total of 3 bridged defects at 12 weeks (Figure 3.3). Similar results were seen with the MSC synthesized ECM: 1 defect bridged by 4 weeks, with an additional defect bridging between 8 and 12 weeks, for a total of 2 bridged defects (Figure 3.4). None of the defects bridged for the collagen coated scaffold group (Figure 3.5).

MicroCT imaging was used to measure the volume of mineralized matrix produced within the central 4.75 mm of the defect site for each limb. The results of this analysis can be seen in Figure 3.6. All groups contained around 5 mm<sup>3</sup> of mineral within the analyzed VOI by 4 weeks. However, due to the large variance within each group, no significant differences were found either between the different groups or between the different time points. Although the difference was not significant, the average volume of mineral within the AFS ECM treated defects at 12 weeks was higher than at 4 weeks and

the other groups at 12 weeks ( $p=0.14$  versus AFS ECM at 4 weeks,  $p=0.18$  versus collagen scaffolds at 12 weeks). Analyses were also done to compare the ECM groups combined to the collagen coated scaffold group. However, no significant difference was found. Images representative of the average volume of mineralized matrix within the defect for each group at each time point can be seen in Figure 3.7.



Figure 3.3: High resolution x-ray images of rat femoral segmental defects treated with AFS synthesized ECM. Images were taken at 4 weeks (left column), 8 weeks (center column), and 12 weeks (right column). Each row corresponds to the same limb at different time points.

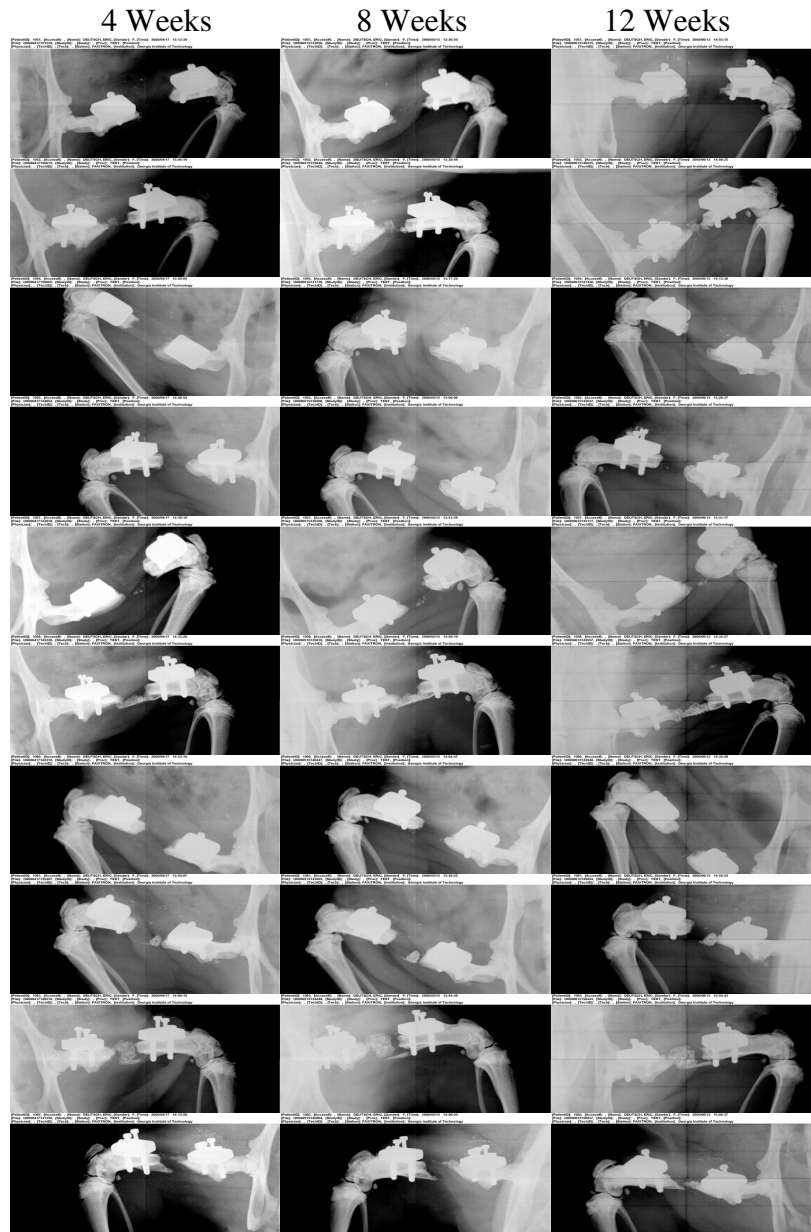


Figure 3.4: High resolution x-ray images of rat femoral segmental defects treated with MSC synthesized ECM. Images were taken at 4 weeks (left column), 8 weeks (center column), and 12 weeks (right column). Each row corresponds to the same limb at different time points.

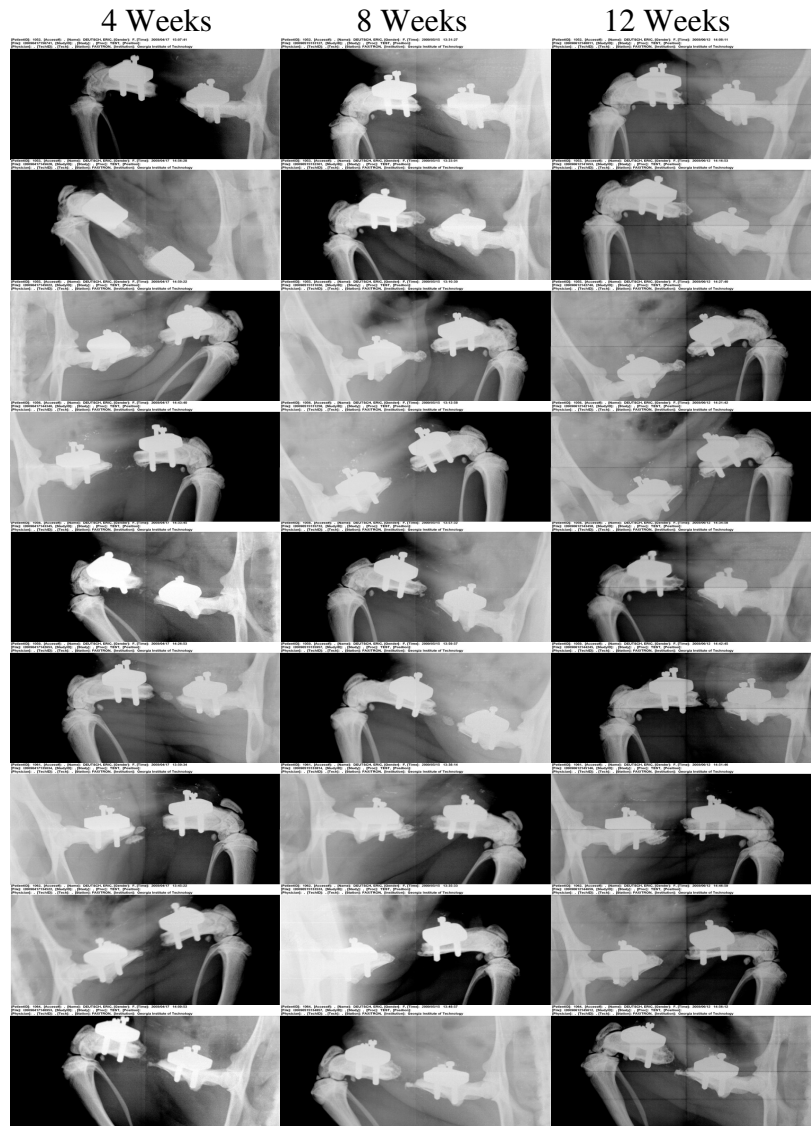


Figure 3.5: High resolution x-ray images of rat femoral segmental defects treated with collagen coated scaffolds. Images were taken at 4 weeks (left column), 8 weeks (center column), and 12 weeks (right column). Each row corresponds to the same limb at different time points.

Table 3.1: Number of bridged defects for each group at each time point, as determined from x-ray images (bridged/total).

Group	Week 4	Week 8	Week 12
AFS ECM	2/10	2/10	3/10
MSC ECM	1/10	1/10	2/10
Collagen	0/9	0/9	0/9

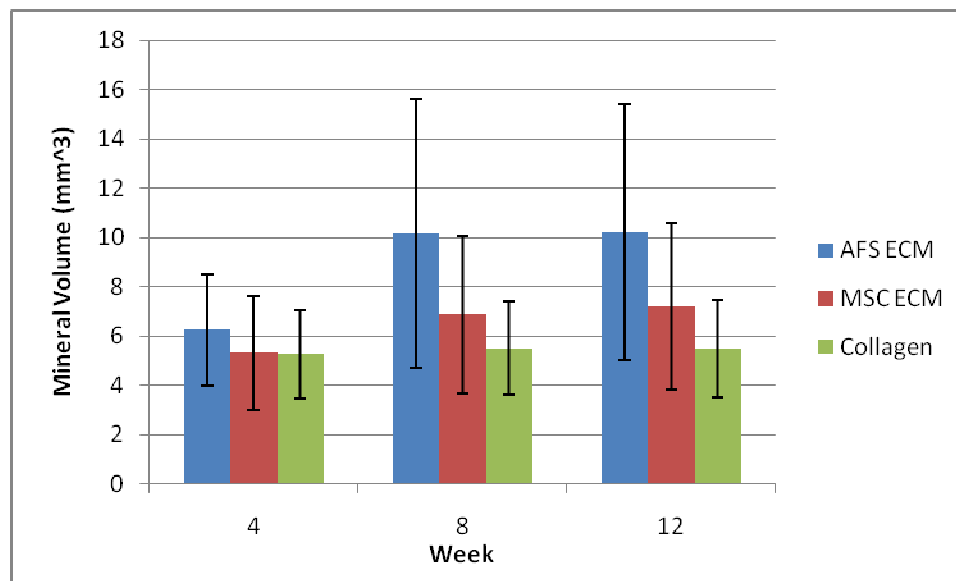


Figure 3.6: Mineral volume within the central 4.75 mm of the a rat femoral segmental defect treated with either AFS cell synthesized ECM, MSC synthesized ECM or collagen coated scaffolds. Error bars are  $\pm$  standard error (n=10 for ECM groups, n=9 for collagen group).



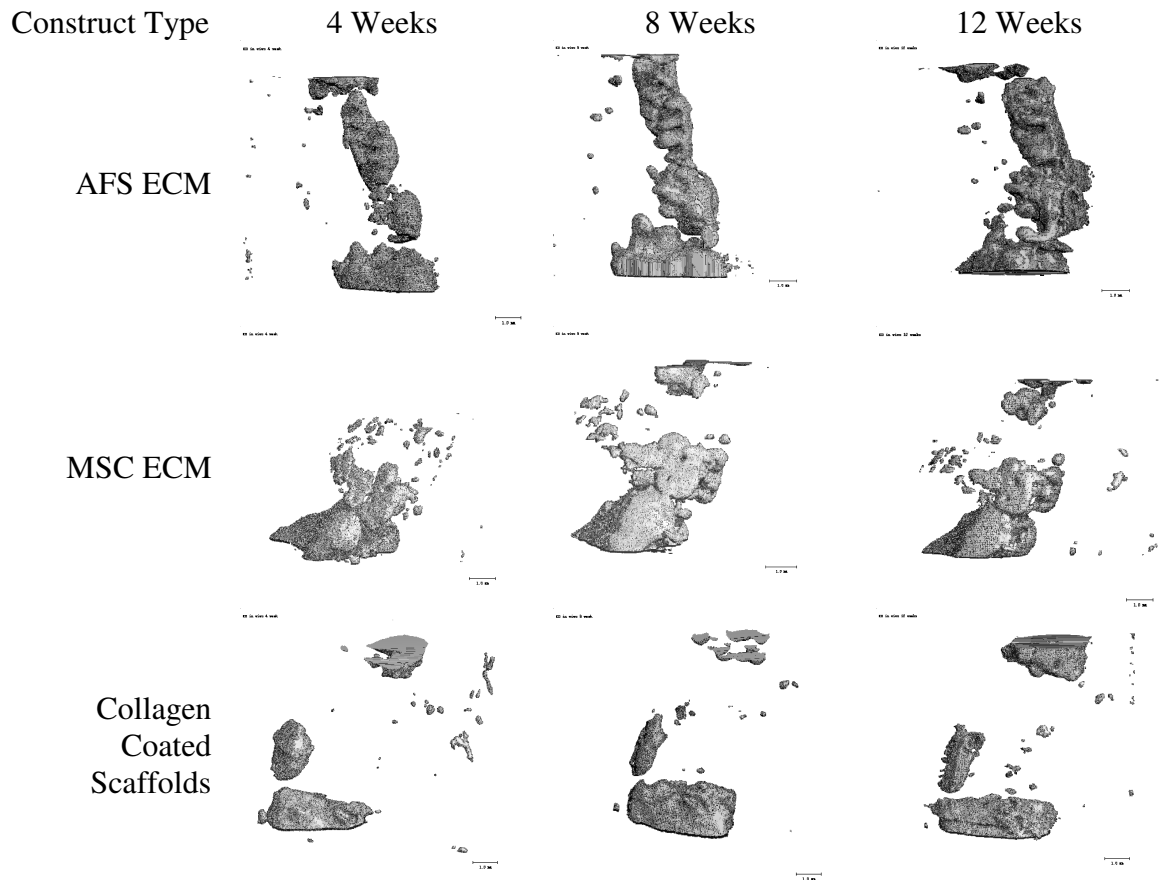


Figure 3.7: *In vivo* microCT images of defects 4, 8, and 12 weeks post-implantation. Images are representative of the average value of mineralized matrix production for each group. Each row shows the same limb at the 3 time points. Scale bar is 1 mm.

## Discussion

An 8 mm femoral segmental defect in a rat provides a challenging test bed for any potential bone tissue engineering therapy. Success in this model is measured by bridging of the defect and the volume of mineralized matrix produced. Both ECM groups performed qualitatively better than the collagen control in terms of bridging. By 12 weeks *in vivo*, 30% of the AFS cell synthesized ECM treated defects, 20% of the MSC synthesized ECM treated defects, and 0% of the collagen scaffold treated defects had bridged. The AFS ECM group had the highest average mineralized matrix volume within the defect site at 12 weeks. However, due to the large variance within each group, this difference was not significant. These results suggest that while ECM did not induce more mineralized matrix production, it may affect the distribution of the matrix within the defect site improving the rate of bridging.

Other potential bone tissue engineering therapies have been tested in this 8 mm rat femoral segmental defect model. Rai et al utilized polycaprolactone-20% tricalcium phosphate scaffolds with platelet-rich plasma. With this treatment, bridging was observed in 5 out of 6 defects.[7] Oest et al combined the growth factors BMP-2 and transforming growth factor  $\beta$ 3 (TGF- $\beta$ 3) with a poly(L-lactide-co-D,L-lactide) to treat the critically sized defect. This treatment resulted in bridging in 2 out of 6 defects. However, even in defects that did not bridge there was a large amount of mineralized matrix formation, with an average volume of over 31 mm<sup>3</sup> at 16 weeks.[6] In comparison to these other results, while the ECM treatments were able to improve the rate of bridging, they fall short of other potential treatments in terms of both rate of bridging and mineralized matrix production.

## References

1. Ishaug-Riley SL, Crane GM, Gurlek A, Miller MJ, Yasko AW, Yaszemski MJ, Mikos AG. *Ectopic bone formation by marrow stromal osteoblast transplantation using poly(DL-lactic-co-glycolic acid) foams implanted into the rat mesentery.* J Biomed Mater Res, 1997. 36(1): 1-8.
2. Byers BA, Guldborg RE, Hutmacher DW, Garcia AJ. *Effects of Runx2 genetic engineering and in vitro maturation of tissue-engineered constructs on the repair of critical size bone defects.* J Biomed Mater Res A, 2006. 76(3): 646-655.
3. Tseng SS, Lee MA, Reddi AH. *Nonunions and the potential of stem cells in fracture-healing.* J Bone Joint Surg Am, 2008. 90 Suppl 1: 92-98.
4. Yasko AW, Lane JM, Fellingner EJ, Rosen V, Wozney JM, Wang EA. *The healing of segmental bone defects, induced by recombinant human bone morphogenetic protein (rhBMP-2). A radiographic, histological, and biomechanical study in rats.* J Bone Joint Surg Am, 1992. 74(7):1111.
5. Lee SC, Shea M, Battle MA, Kozitza K, Ron E, Turek T, Schaub RG, Hayes WC. *Healing of large segmental defects in rat femurs is aided by RhBMP-2 in PLGA matrix.* J Biomed Mater Res, 1994. 28(10): 1149-1156.
6. Oest ME, Dupont KM, Kong HJ, Mooney DJ, Guldborg RE. *Quantitative assessment of scaffold and growth factor-mediated repair of critically sized bone defects.* J Orthop Res, 2007. 25(7): 941-950.
7. Rai B, Oest ME, Dupont KM, Ho KH, Teoh SH, Guldborg RE. *Combination of platelet-rich plasma with polycaprolactone-tricalcium phosphate scaffolds for segmental bone defect repair.* J Biomed Mater Res A, 2007. 81(4): 888-899.
8. Hollinger JO, Kleinschmidt JC. *The critical sized defect as an experimental model to test bone repair materials.* J Craniofac Surg, 1990. 1(1): 60-68.
9. Porter BD, Lin AS, Peister A, Hutmacher D, Guldborg RE. *Noninvasive image analysis of 3D construct mineralization in a perfusion bioreactor.* Biomaterials, 2007. 28(15): 2525-2533.
10. Guldborg RE, Duvall CL, Peister A, Oest ME, Lin AS, Palmer AW, Levenston ME. *3D imaging of tissue integration with porous biomaterials.* Biomaterials, 2008. 29(28)L 3757-3761.

## CHAPTER 4

### CONCLUSIONS AND FUTURE WORK

#### Conclusions

The studies in this thesis were designed to assess the potential of stem cell synthesized extracellular matrix in bone tissue engineering applications. The overall goal was to quantify the osteoinductivity of the ECM produced by human AFS cells, compare it to that of MSCs, and assess its potential for use in bone tissue engineering therapies. To do this, a series of *in vitro* and *in vivo* experiments were designed and executed. First and foremost, the treatment of the ECM with freeze/thaw cycling and DNase was evaluated as a decellularization technique. Next, a series of 2D studies were performed to evaluate markers of osteogenic differentiation for MSCs reseeded on the acellular ECM. Similar studies were also performed to determine the effect of the ECM on the proliferation of the reseeded cells. 3D studies were then performed to determine the effect that the ECM had on reseeded cells in terms of attachment, proliferation, and mineralized matrix production in a more complex 3D environment. Finally, a rat femoral segmental defect model was used to evaluate the use of stem cell synthesized ECM as a bone tissue engineering therapy *in vivo*. It was hypothesized that the ECM produced by the human AFS cells would be osteoinductive, that the degree of osteoinductivity would be greater than that of the MSC-synthesized ECM due to the difference in the initial maturity levels of the cells, and that the mineralization and bridging of defects containing ECM constructs would be greater than that of the empty scaffolds. From the results of these studies, several conclusions can be made:

1. The ECM was successfully decellularized using freeze/thaw cycling and DNase treatment. Following decellularization, the DNA content within 3D PCL/ECM constructs was reduced to less than 10% of the predecellularization value. Any residual DNA in constructs was undetectable after 1 week in culture. Prior to decellularization, live/dead staining showed live cells saturating the scaffolds. After decellularization, no live cells could be found in any region of the construct.
2. Reseeded MSCs were able to attach to and proliferate on both ECM types. Live/dead images showed live cells attached to all regions of the scaffold following reseeding. The attachment efficiency in 3D constructs fell between 25% and 50% for each ECM type and preculture period, significantly less than collagen coated scaffolds. However, the cells were able to proliferate rapidly on each ECM, matching the DNA content of the collagen coated scaffolds by 1 week. DNA content in both 2D and 3D culture increased 5-fold over the first week of culture, illustrating the proliferative potential of the reseeded cells on the ECM.
3. In 2D culture, reseeded cells seeded on ECM synthesized by each cell type showed evidence of osteogenic differentiation. The osteogenic markers were more prevalent with the MSC synthesized ECM, indicating that it may have superior osteoinductivity compared to AFS cell synthesized ECM in 2D culture. Both cultures showed increasing levels of calcium, consistent with mineralized matrix production by osteogenic cells. Calcium levels rose faster for cells cultured on MSC synthesized ECM. Additionally, MSCs cultured on MSC ECM saw a large peak in alkaline phosphatase activity at 1 week not seen in cells cultured on AFS

ECM.

4. Cells cultured with both ECM and the osteoinductive factor dexamethasone experienced a synergistic effect in terms of osteogenic differentiation. These cells showed a more rapid increase in calcium content, and with the MSC ECM, a greater peak value of alkaline phosphatase activity at 1 week when compared to cells cultured without dexamethasone.
5. In 3D *in vitro* culture, the presence of ECM increased the amount of mineralized matrix production. The AFS ECM groups showed higher mineralized matrix volumes than the MSC ECM groups. For the AFS synthesized ECM, the longer preculture period of 8 weeks induced more mineral production than the 4 week period. These results suggest that in 3D, the AFS ECM has the potential to induce more mineralized matrix production, especially with longer preculture periods.
6. Both ECM types contributed to healing of a critically sized rat femoral segmental defect *in vivo*. The rate of bridging was increased with the presence of ECM, with 3 of 10 AFS ECM treated defects and 2 of 10 MSC ECM treated defects bridging, compared to 0 of 9 collagen coated scaffold treated defects. However, there was no significant difference in mineral volume between the ECM groups and collagen coated scaffolds at any time point.

Overall, acellular stem cell synthesized extracellular matrix possesses useful characteristics as a bone tissue engineering therapy. Cells were able to attach to and proliferate on the matrix. Osteoinductive effects were noted in both 2D and 3D *in vitro* culture. The MSC synthesized ECM appeared to have the greater osteoinductive effect in 2D culture with the shorter 3 week preculture period, while the AFS synthesized matrix

had a greater effect in 3D with the longer 8 week preculture period. Both matrix types were able to aid in repair of a bone defect in a clinically relevant model, increasing the rate of bridging of the defects. However, the ECM failed to bridge the majority of the defects or induce mineralized matrix production beyond that seen with a collagen coated scaffold. When compared to the gold standard of BMP delivery, *in vivo* results suggest that the acellular stem cell synthesized extracellular matrix tested here is less effective as a bone tissue engineering therapy. However, the observed effects *in vitro*, particularly the noted synergistic effect, suggest that a therapy that stem cell synthesized ECM combined with another osteoinductive agent may have usefulness as a potential treatment for bone defects.

### **Future Work**

Improvements and further studies have been considered for evaluating the use of stem cell synthesized extracellular matrix as a bone tissue engineering therapy. A pronounced synergistic effect on osteogenic differentiation was noted when the ECM was combined with the osteoinductive agent dexamethasone. Similar results have been seen in other studies.[1, 2] These studies hypothesized that the effect may be due to the ECM providing an optimal microenvironment for osteogenic differentiation. The combined delivery of ECM with another osteoinductive agent, such as BMP-2, may be tested in a segmental defect model to determine if this synergistic effect is also observed *in vivo*. Another interesting approach for including additional osteoinductive agent would be to use gene therapy to cause the cells synthesizing the ECM construct to over express BMP-2 in order to incorporate more of it within the ECM itself. If more bridging and mineralized matrix production are observed with the additional osteoinductive factors, it

is also important to perform mechanical testing on the healed defects to evaluate the restoration of function.

Further *in vitro* characterization of the ECM properties is important if the combined delivery of ECM and osteoinductive agent is successful. This will allow for fine-tuning of the therapy to produce the most desirable effect. One interesting observation to further elucidate would be that the MSC ECM was more osteoinductive in 2D with a 3 week preculture period, while the AFS ECM appeared to be more osteoinductive in 3D with an 8 week preculture period. Two possible explanations for these observations are that either the ECMs from the different cell types perform differently in 2D versus 3D culture, or that they perform differently with different preculture periods. To examine this further, additional preculture time periods can be evaluated in the 3D model.

Once optimal preculture times are established, the composition of the ECM should be examined further. A bicinchoninic acid assay can be performed to measure the total protein content of the ECM and determine if it correlates to mineralized matrix production. Additionally, more complex biochemistry techniques can be used to determine the specific components of the ECM and their relative concentrations.

In addition to further examining the osteoinductive effects, other effects of the ECM on reseeded cells that would be beneficial to bone tissue engineering can be evaluated. In this thesis, the attachment and proliferation of reseeded cells on ECM was examined. It was observed that although fewer cells attached to the ECM than to collagen coated scaffolds, the cells on the ECM constructs proliferated more during the first week, resulting in a DNA content equal to that found in the collagen coated scaffolds after 1



week. However, the observed higher proliferation rate on the ECM constructs may have been due to saturation at the 1 week time point. To further examine this, additional evaluation time points can be added both before and after 1 week to approximate the rate of proliferation on the various scaffold types.

Finally, another potential beneficial effect of the ECM that was not examined in this study is improved angiogenesis. Other studies have found that the presence of MSC synthesized ECM resulted in increased blood vessel formation within an intramuscularly implanted scaffold when compared to an empty scaffold.[3] To evaluate the angiogenicity of the various ECM types, they could be implanted either subcutaneously or in a segmental defect. The blood vessel formation could then be analyzed through both histology and microCT by perfusing the animal with a contrast agent. Further analysis of all of these effects would help fine-tune and improve the use of stem cell synthesized ECM as a bone tissue engineering therapy.

## References

1. Datta N, Holtorf HL, Sikavitsas VI, Jansen JA, Mikos AG. *Effect of bone extracellular matrix synthesized in vitro on the osteoblastic differentiation of marrow stromal cells*. Biomaterials, 2005. 26(9): 971-977.
2. Pham QP, Kasper FK, Scott Baggett L, Raphael RM, Jansen JA, Mikos AG. *The influence of an in vitro generated bone like extracellular matrix on osteoblastic gene expression of marrow stromal cells*. Biomaterials, 2008. 29(18): 2729-2739.
3. Pham QP, Kasper FK, Mistry AS, Sharma U, Yasko AW, Jansen JA, Mikos AG. *Analysis of the osteoinductive capacity and the angiogenicity of an in vitro generated extracellular matrix*. J Biomed Mater Res A, 2009. 88(2): 295-303.